Glide Path Preparation of Nine Instrument Systems and Their Effect on Final Canal Area in Simulated Canals

A THESIS
SUBMITTED TO THE FACULTY OF THE GRADUATE SCHOOL
OF THE UNIVERSITY OF MINNESOTA
BY

David Charles Goerig DDS

IN PARTIAL FULFILLMENT OF THE REQUIREMENTS
FOR THE DEGREE OF
MASTER OF SCIENCE

Dr. Scott McClanahan, Dr. Walter Bowles, Dr. Alex Fok

August 2013

Dedication

To my Parents, Ace and Nancy, for their love and unyielding support

To Shannon for her giving me the strength and support to follow my dreams

To my sons Daniel and Dominic, for whom I work hard now to spend more time with later

Acknowledgements

I would like to express my sincere gratitude to the following people

Dr. McClanahan, Dr. Bowles, Dr. Fok

For your assistance and guidance in helping me complete this study, and for serving on my examining committee

Dr. Nathan Kroll, Jill Balgaard, Robert Henson, Dr. Brian Barsness

Without your help this process would have been intensely challenging to complete. Thank you for your many hours of work.

Mike Creston

For your support, creativity and knowing just what to make, even when I didn't know myself.

The MDRCBB

For your guidance, help and trust. Thank you to all of those friendly folks on the 16th floor who took time out of their day to train me and answer my questions.

Scott Lunos

For your support and skill in statistical analysis.

Abstract

Introduction: This study evaluated glide path preparation of nine instrument systems in simulated S-shaped canals and the preparation's effect, if any, on the two-dimensional surface area after final instrumentation to a clinically relevant size.

Methods: One hundred S-shaped canals were filled with ink and preinstrumentation images were obtained using a stereomicroscope. Glide path preparation was performed by an endodontic resident using FlexoFiles, FlexoFiles mounted in M4 safety handpiece, rotary EndoMagic instruments, rotary K3 instruments, rotary PathFiles instruments, rotary Pre Shaper instruments, rotary ScoutRace instruments, rotary V-Glide instruments, and rotary X-Plorer instruments. Preinsturmentation and postflaring images were superimposed and S-Shaped canals were measured for deviation in both curves. All Blocks were instrumented with K3XF to a final apical size of 35/0.04. Surface areas of preinstrumentation and postinstrumentation images were measured to obtain a percent change for each block and the mean percent change was compared amount groups.

Results: The mean difference of material removed from the apical curvature demonstrated no significant difference between the nine groups ($p=0.3408$), whereas there was a significant difference in means between the groups in the coronal curvature ($p<0.0001$). Comparison of the percent change in mean surface area amongst the groups before and after instrumentation with K3XF were not statistically significant ($p= 0.1782$).

Conclusions: A variety of methods may be employed to obtain a glide path with minimal deviation from the original canal space and that the method used may not have much influence of the final canal shape.

TABLE OF CONTENTS

List of Figures

List of Tables

Introduction

The primary goal of endodontic therapy is prevention and treatment of apical periodontitis. Arguably the most important part of a non-surgical root canal procedure is the preparation of the canal space.(1) The quality of the preparation is determined by instrumentation and mechanical debridement which, subsequently facilitates delivery of irrigants and medicaments, and obturation.(2) Initial scouting of the canal system is a crucial step of the preparation as it allows assessment of the root canal anatomy, much of which cannot be appreciated with conventional radiography. Negotiation of this complex system establishes access to the apical region of the canal creating a path for subsequent instruments to follow. Establishment of a glide path is accomplished by enlargement of this initial path to allow unimpeded access, and can be tedious in constricted or calcified canals. This task is further complicated in canals with severe curvatures or varied anatomy such as fins or apical deltas.

Manual preflaring or glide path is an important prerequisite to shaping with nickel-titanium (NiTi) rotary instruments as it has been shown to reduce instrument fracture (3-6). It is suggested by manufacturers of NiTi systems to secure a glide path up to a size #15 or #20 hand file at working length before using rotary instruments(7). The size of the glide path created before instrumentation has been shown to be inversely related to the amount of torque generated during NiTi instrumentation (8). Over the last five years several manufactures have introduced rotary NiTi instruments of small taper (0.01-0.02) in small sizes (10-20) for the purpose of negotiation and creation of glide path in place of a glide path prepared by hand instrumentation. Although files as small as #15

have been available in 0.02 taper for some time, the PathFile series (Dentsply Maillefer, Tulsa, OK) was specifically designed in intermediate sizes (13/0.02, 16/0.02, 19/0.02; (size/taper) where the size of file is measured at the tip in hundredths of mm) for this role. Initial research by the system's creators have demonstrated less modification to curvature and fewer aberrations when compared to manual (hand file) preflaring with stainless-steel files in simulated S-shaped (double curved) canals independent of the operators endodontic experience level(9). In a μCT study of extracted teeth, PathFiles demonstrated better centering ability than stainless-steel hand files(10). In a randomized clinical trial, the use of PathFiles was associated with reduced post-operative pain compared to manual preflaring with stainless-steel files(11). The author attributed the reduction of pain to less debris extrusion due to the rotary motion of the instruments.

Investigations into the mechanical properties of NiTi glide path instruments have been conducted by two groups in Brazil. Initially Lopes et al. (12) evaluated the buckling resistance of the 13 PathFile (0.13mm) compared to two types #10 hand files. This study was followed by comparisons of mechanical behaviors of the PathFile and Scout RaCe files with pathfinding hand files (13, 14). Together this body of research demonstrates that NiTi instruments are more flexible but less torque resistant than stainless-steel instruments.

A recent study by Ajuz et al. (15) investigates canal deviation in simulated S-shaped canals after negotiation and glide path preparation with PathFile, Scout RaCe and hand K-files. The findings of this study suggest that rotary NiTi instruments promoted less deviation to the original canal anatomy when compared to hand operated

instruments, which is consistent with previous findings for the PathFile (9). Among the files tested the Scout RaCe showed overall significantly better performance. A radiographic comparison of canal transportation in the mesial roots of extracted mandibular molars was conducted by Alves et al. (16). Instruments tested included the PathFile, Mtwo and K-files, none of which demonstrated transportation or aberrations. Radiographic studies have the advantage of instrumentation of actual dentin and impart more clinical relevance due to the difference on hardness compared to resin blocks. However, due to the small size of the instruments, it may be questioned whether or not such small changes would be radiographically evident. The paper does elicit questions regarding clinical relevance of comparison between centering ability or deviation of such small instruments from the original canal space when the final instrumentation will be of a greater size and taper.

To this point, the growing body of literature regarding rotary NiTi glide path instruments has focused on the two systems (PathFile and Scout RaCe). In clinical practice dentists have many options thanks to a competitive market. Pre Shaper, V-Glide and X-Plorer have been recently introduced and marketed as rotary glide path systems. Many systems such as K3 and EndoMagic offer 0.02 taper instruments as small as a tip size of 15 that could be used for creation of a glide path. Clinicians may use a reciprocating handpiece with a head that accept hand files such as the M4 safety handpiece to expedite negotiation to the apical area. The purpose of this study is to evaluate glide path preparation using nine instrument systems in simulated S-shaped

canals and to determine if any of these systems have a significant effect on the final two-dimensional surface area measured in the longitudinal plane.

Review of the Literature

Objectives of Cleaning and Shaping

It is well established that bacteria are the etiology of pulpal and periradicular pathosis (17). The primary goal of endodontics is the prevention of and treatment of periradicular pathosis. Current therapy focuses on the mechanical removal of diseased pulpal tissue and dentin, which facilitates chemical disinfection of the pulp space. Schilder (1) coined the axiom "what comes out is as important as what goes in," emphasizing the flow of an ideal preparation that reflects the original anatomy of the canal and facilitates proper irrigation and obturation. In regards to preparations that are to be obturated with gutta-percha, he outlines five design objectives:

1. Continuously tapering funnel from the apex to the access cavity
2. Cross-sectional diameter should be narrower at every point apically.
3. The root canal preparation should flow with the shape of the original canal.
4. The apical foramen should remain in its original position.
5. The apical opening should be kept as small as practical.

And four biologic objectives:

1. Confinement of instrumentation to the roots themselves.
2. No forcing of necrotic debris beyond the foramen.

3. Removal of all tissue from the root canal space.

4. Creation of sufficient space for intra-canal medicaments.

These objectives remain evident over the evolution of canal shaping techniques, which has seen much growth over the past 40 years. The step-back technique (18, 19), the anti-curvature filing technique (20), the step-down technique (21), and the balanced force technique(22) all relied on stainless-steel instruments to support Schilder's objectives and reduce errors in instrumentation while improving efficiency when shaping the canal system. Common themes such as initial canal scouting, preflaring, and the use of instruments in a rotary motion prevail in modern techniques.

Mechanical preparation of the canal space is accomplished with files and reamers. The use of files in endodontic therapy goes back to 1852 while the K-file commonly used today was introduced in 1915(23). K-type stainless-steel hand files are still a mainstay in endodontic practice today. It has been demonstrated that instrumentation with stainless-steel files can cause aberrations such as zips, elbows (24), ledges or perforation (25) in curved canals. Advances in flexibility, tip design, and technique (360 degree rotary motion vs. filing or reaming) has helped reduce iatrogenic aberrations in the instrumentation of curved or constricted canals.

While hand instruments continue to be used, the introduction of NiTi rotary instruments and other advanced techniques have been widely adopted and avoid some of the major drawbacks of traditional hand instrumentation (23).

Nickel titanium is a super elastic alloy composed of 56% nickel and 44% titanium that exhibits shape memory (26). NiTi instruments were initially investigated by Walia

(27). Instruments made with this alloy demonstrated 2-3 times greater flexibility than stainless-steel instruments. Due to NiTi files' wider range of elastic deformation, it became possible to engineer instruments with greater taper that could be used to instrument curved canals.

Influence and Importance of Creating a Glide Path

During their use in enlarging the canal space, NiTi rotary instruments are subjected to stresses that cause fatigue, which may lead to instrument breakage. Torsional and flexural stresses have been identified as the stresses responsible for fractures. Flexural fatigue may be influenced by work hardening and metal fatigue (28). Torsional stress often occurs in three situations (5):

a) when a large portion of the instrument's surface encounters friction on the canal walls(locking) (29)

b) when the tip of the instrument is larger than that of the canal anatomy to be shaped (3, 30)

c) when excessive pressure is put on the handpiece

Gambarini advocated the use of low (right) torque motors that would allow the clinician to select torque values set below the limit of elasticity for each instrument (30). Despite the almost universal adoption of safer torque controlled motors, torque may rapidly increase beyond the elastic limit resulting in instrument breakage. An initial brief manual instrumentation not only enables torsional stress to be drastically reduced, but also allows the operator the ability to appreciate and understand the original anatomy of

the canal (5). In a study evaluating the number of uses before separation of the Profile Series 29 in extracted teeth (3), only three instruments fractured in the canals prepared with manual preflaring as opposed to 19 in the group without preflaring. A study using simulated canals in resin blocks (5), found that manual preflaring increased by 6-fold the number of blocks instrumented before failure with ProTaper S1. Patino et al. carried out a study designed to specifically evaluate the effect of manual glide path on file separation rate (4). In this study extracted mandibular and maxillary molars with a root curvature greater than 30 degrees were first prepared to a size #20 hand file and then instrumented with either K3, Profile or ProTaper. The number of fractured instruments was compared to a previous study using the same instruments without manual preflaring. Breakage rates were found to be significantly lower (12% vs. 26% respectively) and demonstrated that creation of a glide path before rotary instrumentation was prudent across instrumentation systems.

Rotary Glide Path

Canal Transportation, Deviation, and Centering Ability

Initial investigation of the NiTi rotary glide path instruments compared changes in canal curvature and incidence of canal aberrations after preflaring with either PathFiles or K-type files in S-shape Endo training Blocks (9). 100 blocks were separated into 4 groups with the variables being the two types of instruments and operator experience level. Pre- and post- instrumentation images of the blocks were taken. The images were evaluated for curvature change using animation software to apply a Bezier curve to each image and

evaluate if there was a change in the degree of curvature. There appeared to be a significant difference in the change in curvature between the PathFiles and stainless steel hand files. Canal aberrations were also reduced in the PathFile group. It should be noted that working length was not defined and it appears that all instruments were taken to the terminus of the canal. Evaluation of operator experience showed no statistically significant difference between the inexpert and the specialist groups when PathFiles were used. The data also demonstrated a significant difference between the specialist/hand file group and the inexpert/PathFile group. The author suggests that the PathFile system is less technique sensitive and that an inexpert clinician using the PathFile system may obtain better results than an expert clinician using hand files to obtain a glide path.

Ajuz et al. compared the deviation along S-shaped canals after glide path preparation with hand files, PathFiles and Scout RaCe files (15). The same S-shaped Endo Training Blocks were used as in the Berutti 2009 study. Superimposition of pre- and post-instrumentation images recorded by a CCD camera mounted on a stereomicroscope were used to measure the deviation on either side of the canal at 8 points. Deviation was shown from the canal in all groups. There was a statistically significant difference between the two NiTi rotary groups and the stainless-steel hand files. The authors concluded that NiTi rotary instruments were suitable for preparation of a glide path because they promoted less deviation when compared to stainless steel hand files. It should be noted that the Scout RaCe files were operated at the same settings recommended for the PathFile system (300rpm), which is at least half the rotational speed that is recommended by the manufacture (600-900rpm).

Alves et al. investigated the occurrence of canal transportation and creation of canal aberrations produced by different instruments used to create a glide path in curved mesial canals of extracted mandibular molars (16). The instruments evaluated were stainless-steel hand files (#10,#15,#20), PathFile (13/0.02, 16/0.02, 19/0.02) and Mtwo files (10/0.04, 15/0.05, 20/0.06). The study was conducted using the superimposition of pre and post-instrumentation radiographs. The post-instrumentation radiograph was taken with a #15 stainless-steel hand file in place. They found no canal transportation or aberrations upon review of the images. This is not surprising as it was unlikely that radiographs would be able to adequately demonstrate such small disparities and the choice to use an instrument that was smaller than the last instrument used in any of the groups for radiographic evaluation of transportation is bewildering. Although the choice to attempt to design a more clinically relevant investigation of canal deviation was well intentioned, this technique may be better suited for larger files where greater deviations are likely to occur.

In another study coauthored by the creators of PathFile, µCT was used to evaluate the PathFiles' ability to remain centered in the canal compared to manual preflaring with hand files (10). The study design provides a non-destructive means to evaluate instrumentation on actual dentin and was therefore more clinically relevant than the use of simulated canals. The drawbacks tend to be expense and the time consuming nature of scanning, reconstruction and evaluation. As a result, sample size tends to be much lower. Eight extracted maxillary molars were used in this study; scans were taken before and after instrumentation. Pre- and post-scans were evaluated for diameter ratios and the ratio

of cross-sectional areas at various points. The authors concluded that the PathFile significantly reduced canal modifications confirming previous studies.

Mechanical Properties of Rotary Glide Path Instruments

Endodontic hand instruments used for purposes of negotiating the canal system are typically small (ISO #6-10) and possess the properties that facilitate progression in the apical direction safely (13). Variations in metal composition and design directly influence an instruments behavior and safety. Instruments used to enlarge the glide path should maintain the original canal geometries (31).

Initially Lopes et al. (12) evaluated the buckling resistance of the 0.13 PathFile compared to two types #10 hand files. Unsurprisingly, the PathFile was far less resistant to buckling than the hand files due to metallurgical differences. The study however echoes the importance of buckling resistance in pathfinding instruments suggested by Allen et al. (31) and utilizes an easily reproducible method for evaluation. Force was applied axially until the moment of bending was observed. This is far more clinically relevant than applying a load perpendicular to the file as previously reported (31). This study was followed by another with the same author, evaluating of mechanical behaviors of the C-Pilot (VDW), PathFile and Scout RaCe, which included resistance to bending and buckling, cyclic fatigue and torsional load (13). Their findings included a significant difference in the buckling resistance test between all file types. PathFiles were the most resistant to cyclic fatigue, with the Scout RaCe demonstrating the lowest torque to fracture. It was the conclusion of the authors that *the different mechanical behavior of the*

instruments in the different tests indicates that the combined use of stainless-steel hand instruments and rotary NiTi instruments during the exploration of narrow curved canals may be necessary to exploit the best performance of each pathfinding instrument.

Nakagawa investigated resistance to bending, torsional resistance, Vickers microhardness, alloy composition as well as instrument design elements of the PathFile, Scout RaCe and RaCe ISO 10 files (14). Evaluation confirmed that all instruments were compatible with the manufactures' definition and were within the accepted ISO tolerance limits. According to the results it was apparent that instrument design and dimensions (size and taper) play an important role in determining flexibility but cannot describe the influence of instrument geometry of the flexibility. This is to say that across file systems of similar dimensions mechanical properties were different despite having the same chemical composition and tapers. In agreement with other studies the NiTi instruments were found to be more flexible that K-type files and may more effectively maintain the original path during instrumentation of curved canals.

Clinical Studies

A randomized clinical trial was conducted including 295 patients receiving root canal therapy(11). In half of the patients, manual preflaring was performed with K files to a #20 prior to instrumentation with NiTi rotary instruments. The other half received preflaring with PathFile instruments before instrumentation with NiTi instruments. Patients were evaluated for post-operative pain levels as well as intake of analgesics. Patients in the PathFile group showed less time to pain resolution as well as lower

postoperative analgesic intake. The author contributed the results to reduction of debris extrusion as a result of the PathFiles' use in rotary motion compared to the filing motion in the hand instrumentation group. The author concludes *that performing a glide path with hand instrumentation may have a significant impact on individual quality of life in terms of postoperative pain, and the use of NiTi rotary instrumentation may be rather beneficial.* (11)It should be of note that although the authors explicitly deny any conflicts of interest related to this study in the acknowledgements, the creators of the PathFile are coauthors of this paper and a retraction had to be printed several months later.

Hypothesis

The null hypothesis of this study is that the means of obtaining a glide path had no influence on the final shape of the canal after instrumentation of the canal to a clinically relevant size.

The alternative hypothesis of this study is that the method used for creating of a glide path will cause such a meaningful deviation from the original canal geometry that it will influence the shape of the final canal after instrumentation of the canal to a clinically relevant size.

Materials and Methods

Preparation of Samples

One hundred five ISO #15, 0.02-tapered, S-shaped Endo Training Blocks (Dentsply Maillefer, Tulsa, OK) were used in this study. The blocks were each indexed

with two cylindrical spaces to the depth of 5mm. The depth was consistent with the same plane as the simulated canal, which allowed for the index to be in focus when images were recorded. A custom jig was fabricated from aluminum and consisted of a custom notch which held each S-shaped block. On the reverse side of the jig was a guide that limited the corresponding drill bit's depth of penetration. The drill bit was 2.3619mm in diameter, and modified with a soldered ring. The cylindrical index's consistent diameter, depth and unique crisp appearance in the focal plane aided calibration and alignment during superimposition of pre- and post- instrumentation images.

Blocks to be instrumented with rotary glide path instruments were assigned a number of 1-90. Ten blocks were set aside as positive controls, which would receive only instrumentation with K3XF with no preflaring. Five blocks acted as the negative controls and did not receive any shaping and were used to check the validity of the superimposition and processing of compiled images. A random preparation order was created for the nine groups using a random numbers table. This was done to limit the bias of operator fatigue, ensure block distribution was fair, and to conceal the preparation group from the evaluators. A master list was kept by the primary operator (DG) so that he could know which instrument system to use on which block and to correlate the data for statistical analysis.

Methylene blue dye was injected into the simulated canal space with a tuberculin syringe. The block was then mounted 90 degrees to the objective lens on the same jig used for indexing which was secured to the base of an Olympus MVX10 stereomicroscope (Olympus America, Melville, NY). Pre-instrumentation images were

taken using acquisition software (MicroSuite Five, Olympus America, Melville, NY) with and Olympus DP71 CCD Camera (Olympus America, Melville, NY) attached to the microscope at 40x magnification. Images were saved in .jpg format at a resolution of 4080x3072 at 300dpi.

Instrumentation

Characteristics of representative instruments for each system were inspected (Appendix IV). Images of the tip and apical 3mm were acquired using a TM3000 scanning electron microscope (Hitachi, Tokyo, Japan). The file that closely corresponded to a #15 in each system was embedded in epoxy (Loctite, Westlake, Ohio), sectioned at D3 and the cross section was imaged using the same criteria as above.

All instruments were sterilized before use. All instruments were only used in a single canal. The working length (WL) was determined to be 16mm, which was found to correspond to approximately 0.5mm short of the terminus. Before instrumentation, a #10 K-Type file was taken to the terminus of the canal to ensure patency. Instruments were used at rotational speeds suggested by their manufacturer, when a range was given; the mean of the recommendation was used. Dye in the canal served as lubricant during the preflaring instrumentation and was replenished if necessary.

In the hand file group, #10,15 and 20 K-type FlexoFiles (Dentsply Maillefer, Tulsa, OK) were used in that order to WL. The #10 and 15 were used in a watch-winding pull motion whereas the #20 was used in a combination of watch-winding and balanced force. The M4 group utilized the same K-type files as the hand file group. The

instruments were taken to working length in ascending order after insertion into handpiece of the M4 Safety motor(Sybron, Orange, CA). The torque controlled motor used to drive the M4 handpiece and for all of the NiTi rotary groups was an Endo ITR Endodontic Motor (Aseptico Inc, Woodlinville, WA). The torque setting was set to 3 and was used for all instruments. The hand piece used for all NiTi rotary instruments was Nouvag TCM 8:1 contra angle (Nouvag, Lake Hughes, CA). The EndoMagic (Endo Solutions York, PA)group included a 15/0.02 and 20/0.02 at rotational speed 350rpm. The K3(Sybron, Orange, CA) group included a 15/0.02 and 20/0.02 at rotational speed 350rpm. The PathFile (Dentsply Maillefer, Tulsa, OK) group included a 13/0.02, 16/0.02 and 19/0.02 at rotational speed 300rpm. The Pre Shaper (Specialized Endo, Portland, OR) group included a 14/0.02 and 18/0.02 at rotational speed 500rpm. The Scout RaCe (Brasseler, Savannah, GA) group included a 10/0.02, 15/0.02 and 20/0.02 at rotational speed 750rpm. The V-Glide (SSWhite, Lakewood, NJ) group included a 13/0.02 and 17/0.02 at rotational speed 300rpm. The X-Plorer (Clinicians Choice, New Milford, CT) group included a 15/0.01, 20/0.01 and 20/0.02 at rotational speed 400rpm. Following creation of glide path, dye was replenished and a post-flaring image was captured as described above.

After glide path creation and image capture, all s-blocks were subject to instrumentation with the K3XF with a final size of 35/.04. Introduction of a tenth group provided a control group that did not receive preflaring before instrumentation with the K3XF. These blocks were inserted every 10^{th} block into the prep order to ensure they were not all instrumented at once with bias accounting to operator fatigue. All samples

were instrumented according to the manufactures directions for use. This included a crown down technique consisting of 40/0.04, 35/0.04, 30/0.04, 25/0.04. Each file progressed apically until resistance was met and then withdrawn and the flutes were cleaned by inserting into a sponge and inspected for deformation. Irrigation with tap water was used between files as well as maintenance of patency by passing a #10 hand file no more than 0.5mm past the foremen. Unlike the glide path instruments, the K3XF instruments were used for no more than 3 canals and were discarded if unwinding occurred. Upon reaching an apical prep size of 35/.04 the canal was rinsed and dye was injected. A post-instrumentation image was captured as described above.

Preparation of Images for Measurement of Resin Removed

Photoshop (CS6 extended Adobe systems Inc., San Jose, CA) was used to superimpose pre-instrumentation and post-flaring images for each sample. Both pre-instrumentation and post-flaring images were opened in Photoshop using the load files into stack with auto-align option selected. The images were loaded into two layers and proper alignment was confirmed. The pre-instrumentation canal was selected using the quick selection tool. The selection was inverted and the background was deleted from that layer. The color of the pre-instrumented canal was inverted so that contrast between the uninstrumented canal and the flared canal could be distinguished (Figure 1).

(Figure 1) Superimposition of pre-instrumentation (white) and post-flaring (black). (Hand File)

The resulting image was rotated and cropped so that the terminus was vertical and corresponded with the leftmost border of the image. It was then saved with a sample ID to be measured by two evaluators. Superimposed images can be found in appendix C arranged by group.

Measurement of Resin Removed

An image containing a calibrated measurement from the microscope acquisition software was used to determine a pixel/mm ratio of (473pixels/1mm). Measurements were made by two independent reviewers using the ruler tool in Photoshop CS6 extended. Images were enlarged to 400% and viewed at 2560x1600 resolution on a HPZR30w LCD monitor (Hewlett-Packard, Palo Alto, CA). Reviewers were limited to no longer than 1.5 hours of working time before being mandated to take a 15-minute

break to reduce fatigue. They were also limited to no more than 3 hours of working time per day. Both reviewers were blinded to which sample belonged to which group. Measurements were made perpendicular to the original canal from both the top and bottom of the canal at 1mm, 2mm, 3mm, 4mm, 5mm, 6mm and 7mm. An average of both reviewers' measurements was used for all calculations. Inter-reviewer reliability was assessed by taking the difference between the means of the two evaluators' for all fourteen-measurement levels (Table 3). The average of the difference between them was 0.002 and that was an acceptably low value. The reviewers returned a week after completion of initial measurements and re-measured ten randomly chosen samples for the purpose of evaluating intra-reviewer reliability. To determine the intra-reviewer reliability, each measurement was subtracted from the original measurement and an average was taken for each evaluator (Table 4). Both evaluators had an intra-rater reliability value of 0.001.

The tendency to deviate toward the inner aspect of the curve was calculated for both curves for each group by subtracting the average depth of material removed from the outer portion of the curve from that of the internal aspect of the curve at four points. The apical curve (curve 1) included the mean difference at points 1mm, 2mm, 3mm, 4mm and the coronal curve (curve 2) included the mean difference at points 4mm, 5mm, 6mm and 7mm(Figure 2). Because the 4mm measurement was in the junction between the 2 curves it was used in calculating the mean material removed for both curves.

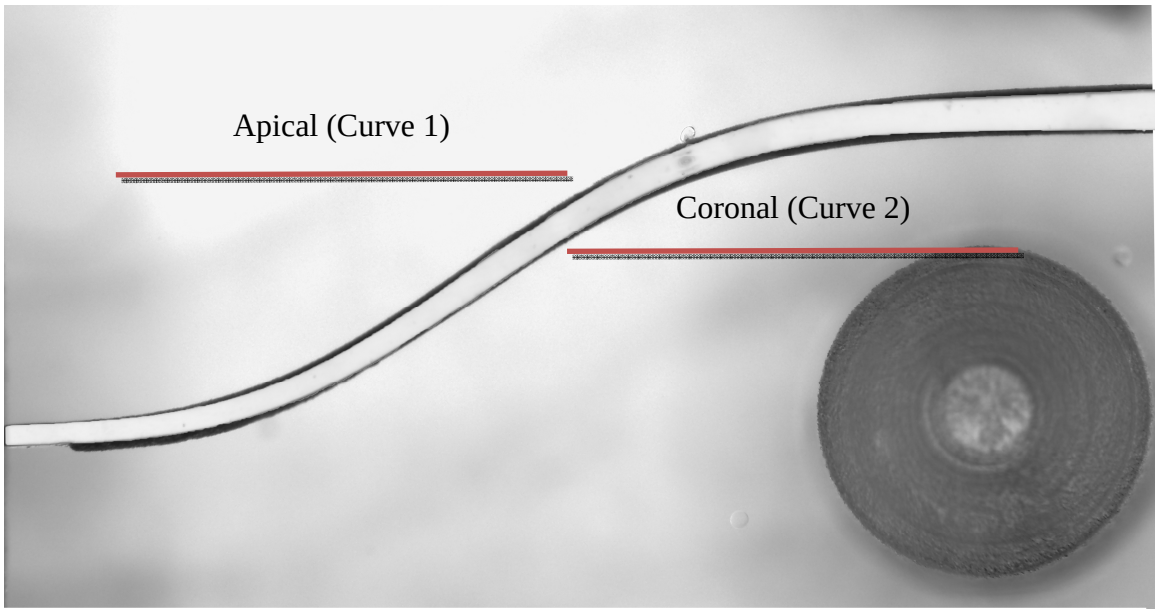

(Figure 2) Measurement locations and distinction of apical and coronal curves. (Pre Shaper)

Preparation of Images and Measurement of Surface Area

Pre-instrumentation images and post-instrumentation images were cropped to a length of 8mm from the apical terminus using Photoshop. A single reviewer (BB) measured the two-dimensional surface area in the longitudinal plane using the quick selection tool for each image. (Table 7) The reviewer was unaware as to which sample belonged to which group. The percent change in surface area was calculated (((post-inst SA - pre-inst SA)/pre-inst SA)x100) for each sample. The mean value of the percent change for the groups was analyzed for variance using the ANOVA test.

Statistical Analyses

The average of the first measurements (by the two raters) was used for the analyses. Descriptive statistics (means, standard deviations, ranges) were calculated for

the 7 difference measurements, as well as the summary outcome measures (curve 1 and curve 2). One-way analysis of variance (ANOVA) was used to compare the mean outcome measure between the 9 groups for each summary outcome. If the overall ANOVA was statistically significant at the 0.05 level, pairwise comparisons were made using a Tukey multiple comparison adjustment. P-values less than 0.05 were considered statistically significant. SAS V9.3 (SAS Institute, Inc., Cary, NC) was used for the analyses. Inter- and intra-measurer errors were also assessed.

Results

The results of the calculation of tendency to deviate for each curve can be found in Table 6. Note that a negative value indicates that preparation deviated toward the outer aspect of the curve. The mean difference of material removed from the apical curvature (curve 1) demonstrated no significant difference between the nine groups (p=0.3408; Figure 3). The hand file group tended to show greater variation then the other groups at this curvature, but this was not statistically significant. K3 SR X had means closest to zero (Table 6).

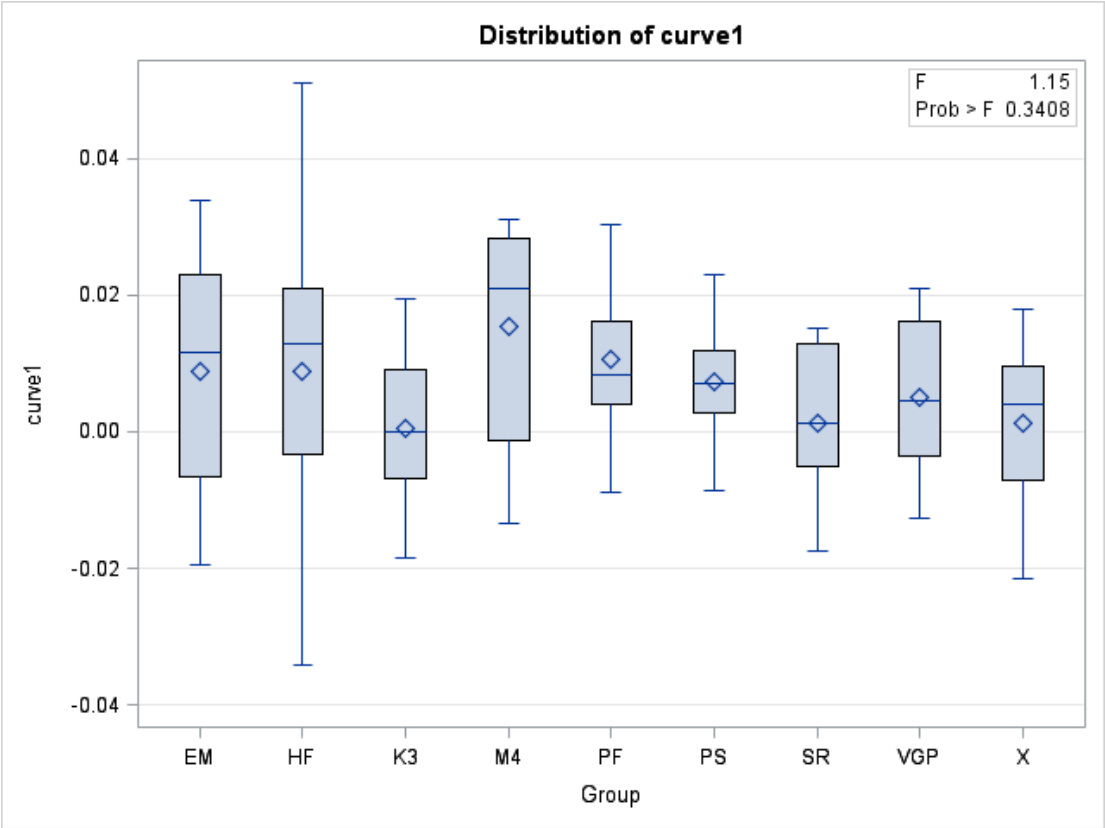

(Figure 3) Mean difference of material removed for curve 1 by group

The mean difference of material removed from the coronal curvature (curve 2) showed a statistically significant difference in means ($p<0.0001$; Figure 4) and pairwise comparisons were made. (Figure 5 & 6) The hand file group deviated more than any group at this level, which was statistically significant when compared to all of the NiTi rotary groups, but not when compared to the M4 group (Figure 5 & 6).

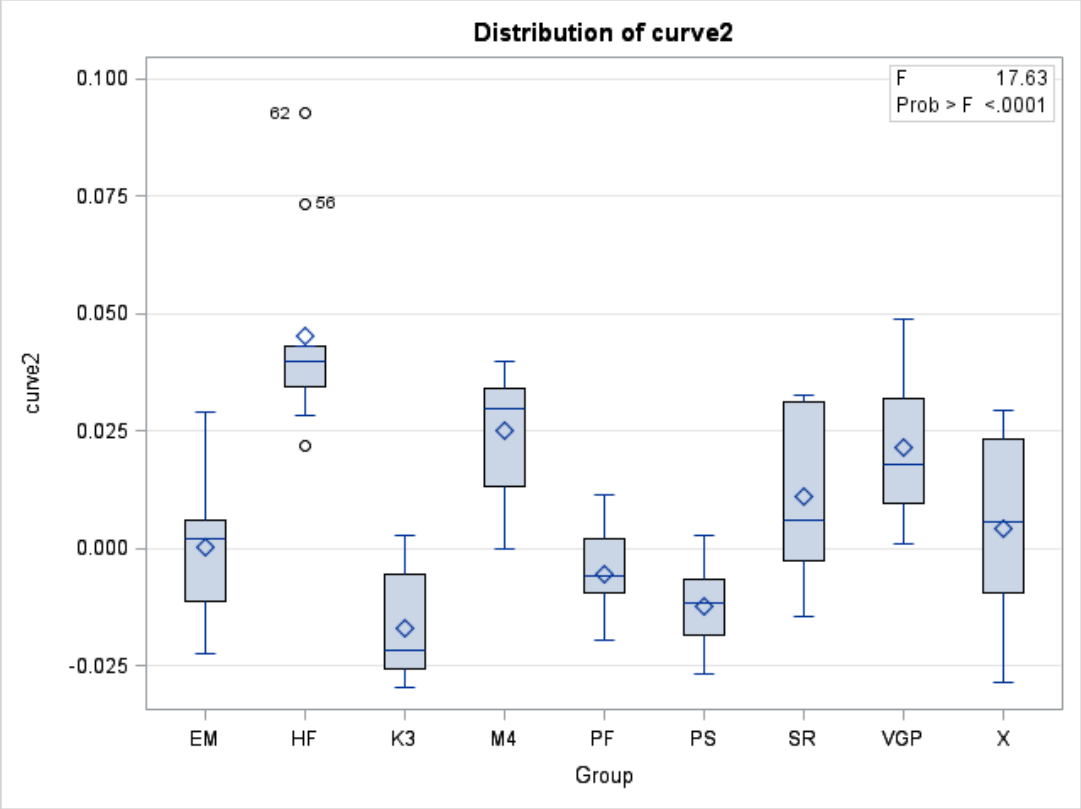

(Figure 4) Mean difference of material removed for curve 2 by group

P-values from pairwise comparisons (Tukey adjustment)
Dependent Variable: curve2

	EM	HF	K3	M4	PF	PS	SR	VGP	X
EM									
HF	**<.0001**								
K3	0.2128	**<.0001**							
M4	**0.0102**	0.0809	**<.0001**						
PF	0.9963	**<.0001**	0.7021	**0.0006**					
PS	0.6431	**<.0001**	0.9984	**<.0001**	0.9793				
SR	0.7807	**<.0001**	**0.0020**	0.4883	0.2740	**0.0207**			
VGP	0.0512	**0.0177**	**<.0001**	0.9998	**0.0044**	**<.0001**	0.8332		
X	0.9995	**<.0001**	**0.0498**	0.0606	0.8868	0.2615	0.9822	0.2173	

(Figure 5) Pairwise comparison of curve 2

Means with the same letter are not significantly different.

Tukey Grouping				Mean	N	Group
		A		0.045101	10	HF
		A				
B		A		0.025005	10	M4
B						
B		C		0.021332	10	VGP
B		C				
B		C	D	0.011025	10	SR
B		C	D			
B	E	C	D	0.004154	10	X
	E	C	D			
F	E	C	D	0.000056	10	EM
F	E		D			
F	E		D	-0.005352	10	PF
F	E					
F	E			-0.012389	10	PS
F						
F				-0.017192	10	K3

(Figure 6) Pairwise comparison of curve 2

The mean percent change in surface area for each group can be found in Table 7 (appendix I). Comparison of the percent change in mean surface area amongst the groups before and after instrumentation with K3XF were not statistically significant (p= 0.1782; Figure 7).

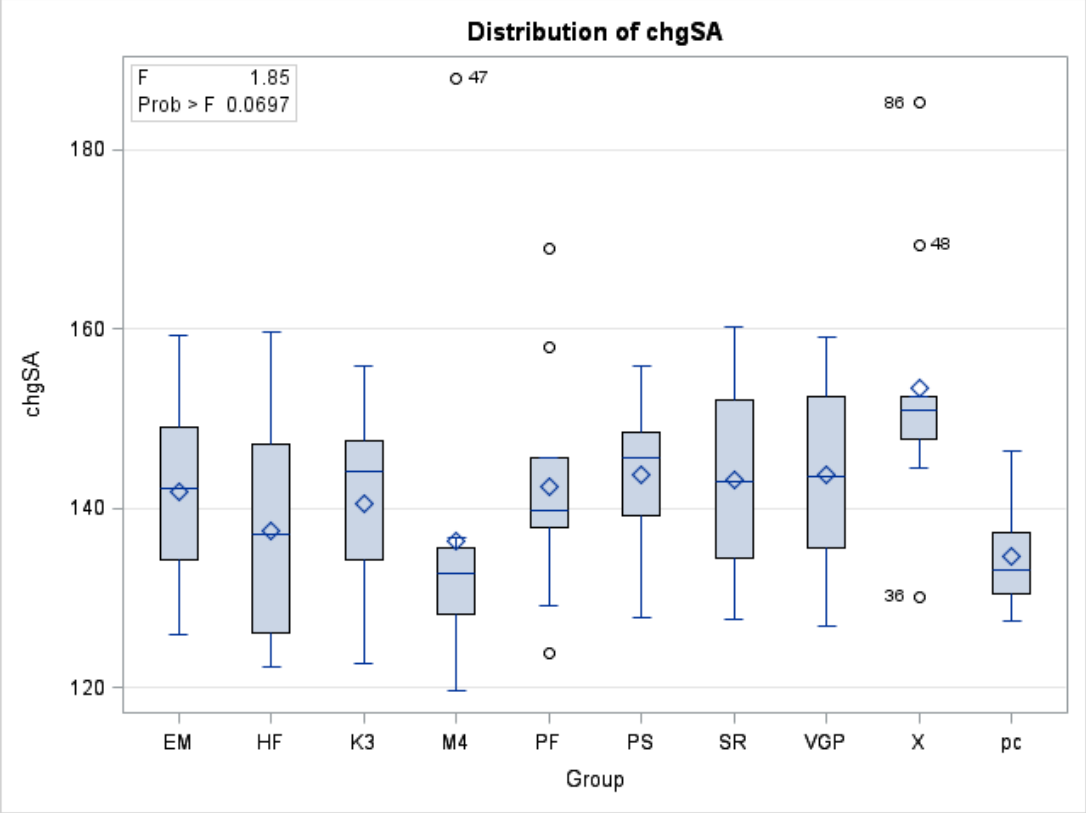

(Figure 7) Pairwise comparison of curve 2

Discussion

Several investigations on the shaping ability of instruments and techniques have been conducted using simulated canals in resin block. Most notably are those using the Cardiff experimental design which employs both 20 degree and 40 degree curvatures either eight or twelve millimeters from the orifice (23). This standardized model has provided a wealth of information for comparison of continuously advancing techniques and instrument designs. The use of simulated canals allows for standardization of the degree and locations of curvature and width of canals as well as excellent visualization analysis of deviations or aberrations. It has been demonstrated as a valid model for

studying the preparation of canals when compared to the natural tooth (32). Despite the advantages this method has its limitations. Evaluation is limited to the longitudinal plane. Canal shaping rather than canal cleaning ability is the objective of analysis. The microhardness of resin tends to be about half that of dentin near the pulp space (32). The composition of debris created during shaping may lead to a higher incidence of blockage. Therefore data regarding working time and safety may not be as transferable to clinical practice as that of studies using extracted teeth.

The S-shaped Endo Training Block was used in this study. One advantage of this block is that it is commercially available and offers standardization amongst researchers worldwide. The s-shape (double curve) offers inherent difficulties that simulate challenges clinicians encounter on difficult cases where they rely on the properties of both their instruments and technique. The S-shape has been shown to influence cyclic fatigue by reducing the number of cycles to fracture when compared to single curved canals (33). A disadvantage of the S-Shaped Endo Training Block in the current study was that the canal size was manufactured at approximately #15/0.02. This is larger than the initial file size in many of the systems evaluated. The block itself is essentially already a glide path that needs to be enlarged. Clinically this may not be relevant as the average size of the mesial canals of mandibular molars one millimeter coronal to the foremen is 200-400 microns (34).

All systems evaluated in this study showed minimal deviation in the apical curvature. The fact that there was not a statistically significant difference between the hand file group and the M4 group in the tendency to deviate toward the inner portion of

the coronal curve is not surprising as both used the same stainless-steel FlexoFiles. This is likely attributed to the higher modulus of elasticity demonstrated by stainless-steel alloy. File design and mode of cutting action (e.g. filing vs. rotary) also may have played a role. What is more surprising is that the M4 group was not statistically different from the V-Glide, Scout RaCe or X-plorer groups in its tendency to deviate toward the inner portion of the coronal curve. This may be in part due to the reciprocating motion of the M4 handpiece. The fact that in three of the groups (PathFile, Pre Shapers, and K3) negative values were seen means that they deviated toward the outer portion of the coronal curve.

Although there was a statistically significant difference amongst the groups in the tendency to deviate in the coronal curve, this has less impact when Shilder's first design objective is met by the subsequent shaping of the canal. All of the final glide path instruments in this study had a taper of 0.02. The final preparation shape provided a continuously tapering funnel of a 0.04 taper. Because all of the samples were instrumented to the same size, a direct comparison of surface area could be made. Due to the inherent variability of the blocks, however small, comparison was made using a percent change in surface area. The data suggests that how the glide path was obtained had no statistically significant influence of the percent change in surface area of the final instrumentation.

Conclusion

Within the limits of this study, it appears that a variety of methods may be employed to obtain a glide path with minimal deviation from the original canal space and that the method used may not have much influence on the final canal shape.

References

1. Schilder H. Cleaning and shaping the root canal. Dent Clin North Am. 1974;18(2):269-96.

2. Peters OA. Current challenges and concepts in the preparation of root canal systems: A review. J Endod. 2004 8;30(8):559-67.

3. Roland DD, Andelin WE, Browning DF, Robert Hsu G, Torabinejad M. The effect of preflaring on the rates of separation for 0.04 taper nickel titanium rotary instruments. J Endod. 2002 7;28(7):543-5.

4. Patino PV, Biedma BM, Liebana CR, Cantatore G, Bahillo JG. The influence of a manual glide path on the separation rate of NiTi rotary instruments. J Endod. 2005 Feb;31(2):114-6.

5. Berutti E, Negro AR, Lendini M, Pasqualini D. Influence of manual preflaring and torque on the failure rate of ProTaper rotary instruments. J Endod. 2004 Apr;30(4):228-30.

6. Ehrhardt IC, Zuolo ML, Cunha RS, De Martin AS, Kherlakian D, de Carvalho MCC, et al. Assessment of the separation incidence of mtwo files used with preflaring: Prospective clinical study. J Endod. 2012 8;38(8):1078-81.

7. Ruddle CJ. The ProTaper endodontic system: Geometries, features, and guidelines for use. Dent Today. 2001;20(10):60-7.

8. Ha JH, Park SS. Influence of glide path on the screw-in effect and torque of nickel-titanium rotary files in simulated resin root canals. Restor Dent Endod. 2012 Nov;37(4):215-9.

9. Berutti E, Cantatore G, Castellucci A, Chiandussi G, Pera F, Migliaretti G, et al. Use of nickel-titanium rotary PathFile to create the glide path: Comparison with manual preflaring in simulated root canals. J Endod. 2009 Mar;35(3):408-12.

10. Pasqualini D, Bianchi CC, Paolino DS, Mancini L, Cemenasco A, Cantatore G, et al. Computed micro-tomographic evaluation of glide path with nickel-titanium rotary PathFile in maxillary first molars curved canals. J Endod. 2012 Mar;38(3):389-93.

11. Pasqualini D, Mollo L, Scotti N, Cantatore G, Castellucci A, Migliaretti G, et al. Postoperative pain after manual and mechanical glide path: A randomized clinical trial. J Endod. 2012 Jan;38(1):32-6.

12. Lopes HP, Elias CN, Mangelli M, Lopes WSP, Amaral G, Souza LC, et al. Buckling resistance of pathfinding endodontic instruments. J Endod. 2012 3;38(3):402-4.

13. Lopes HP, Elias CN, Siqueira Jr JF, Soares RG, Souza LC, Oliveira JCM, et al. Mechanical behavior of pathfinding endodontic instruments. J Endod. 2012 10;38(10):1417-21.

14. Nakagawa RKL, Alves JL, Buono VTL, Bahia MGA. Flexibility and torsional behaviour of rotary nickel-titanium PathFile, RaCe ISO 10, scout RaCe and stainless steel K-file hand instruments. Int Endod J. 2013:n/a,n/a.

15. Ajuz NCC, Armada L, Gonçalves LS, Debelian G, Siqueira Jr. JF. Glide path preparation in S-shaped canals with rotary pathfinding nickel-titanium instruments. J Endod. 2013 4;39(4):534-7.

16. Alves Vde O, Bueno CE, Cunha RS, Pinheiro SL, Fontana CE, de Martin AS. Comparison among manual instruments and PathFile and mtwo rotary instruments to create a glide path in the root canal preparation of curved canals. J Endod. 2012 Jan;38(1):117-20.

17. Kakehashi S, Stanley HR, Fittzgerald RJ. The effects of surgical exposures of dental pulps in germ-free and conventional laboratory rats. Oral Surg Oral Med Oral Pathol. 1965 Sep;20:340-9.

18. Clem WH. Endodontics: The adolescent patient. Dent Clin North Am. 1969 Apr;13(2):482-93.

19. Mullaney TP. Instrumentation of finely curved canals. Dent Clin North Am. 1979 Oct;23(4):575-92.

20. Abou-Rass M, Frank A, Glick D. The anticurvature filing method to prepare the curved root canal. The Journal of the American Dental Association. 1980 November 01;101(5):792-4.

21. Goerig AC, Michelich RJ, Schultz HH. Instrumentation of root canals in molar using the step-down technique. J Endod. 1982 12;8(12):550-4.

22. Roane JB, Sabala CL, Duncanson Jr. MG. The “balanced force” concept for instrumentation of curved canals. J Endod. 1985 5;11(5):203-11.

23. Hülsmann M, Peters OA, Dummer PMH. Mechanical preparation of root canals: Shaping goals, techniques and means. Endodontic Topics. 2005;10(1):30-76.

24. Weine FS, Kelly RF, Lio PJ. The effect of preparation procedures on original canal shape and on apical foramen shape. J Endod. 1975 8;1(8):255-62.

25. Jafarzadeh H, Abbott PV. Ledge formation: Review of a great challenge in endodontics. J Endod. 2007 10;33(10):1155-62.

26. Thompson SA. An overview of nickel?titanium alloys used in dentistry. Int Endod J. 2000;33(4):297-310.

27. Walia H, Brantley WA, Gerstein H. An initial investigation of the bending and torsional properties of nitinol root canal files. J Endod. 1988;14(7):346-51.

28. Sattapan B, Nervo G, Palamara J, Messer H. Defects in rotary nickel-titanium files after clinical use. J Endod. 2000 MAR;26(3):161-5.

29. Blum J, Cohen A, Machtou P, Micallef J. Analysis of forces developed during mechanical preparation of extracted teeth using profile NiTi rotary instruments. Int Endod J. 1999 JAN;32(1):24-31.

30. Gambarini G. Rationale for the use of low-torque endodontic motors in root canal instrumentation. Dental Traumatology. 2000;16(3):95-100.

31. Allen MJ, Glickman GN, Griggs JA. Comparative analysis of endodontic pathfinders. J Endod. 2007 6;33(6):723-6.

32. Lim KC, Webber J. The validity of simulated root canals for the investigation of the prepared root canal shape. Int Endod J. 1985 Oct;18(4):240-6.

33. Al-Sudani D, Grande NM, Plotino G, Pompa G, Di Carlo S, Testarelli L, et al. Cyclic fatigue of nickel-titanium rotary instruments in a double (S-shaped) simulated curvature. J Endod. 2012 7;38(7):987-9.

34. Green EN. Microscopic investigation of root canal diameters. J Am Dent Assoc. 1958 Nov;57(5):636-44.

Appendix I

Reviewer 1(JB) measurements: The MEANS Procedure

Table 1

Variable	Label	N	Mean	Std Dev	Minimum	Maximum
top1	top1	90	0.0242106	0.0102804	0.0068990	0.0550290
top2	top2	90	0.0594703	0.0231563	0.0217510	0.1417450
top3	top3	90	0.0661035	0.0225132	0.0325990	0.1388390
top4	top4	90	0.0523121	0.0198276	0.0201130	0.1488440
top5	top5	90	0.0399806	0.0136377	0.0087260	0.0694410
top6	top6	90	0.0502020	0.0137921	0.0109080	0.0767190
top7	top7	90	0.0732602	0.0123315	0.0490890	0.1048100
bottom1	bottom1	90	0.0594737	0.0184502	0.0101770	0.1169320
bottom2	bottom2	90	0.0326812	0.0140961	0.0063710	0.0685810
bottom3	bottom3	90	0.0260678	0.0117284	0.0075200	0.0559170
bottom4	bottom4	90	0.0552773	0.0242026	0.0158730	0.1144630
bottom5	bottom5	90	0.0796659	0.0358396	0.0288830	0.1798130
bottom6	bottom6	90	0.0683356	0.0277364	0.0238150	0.1534760
bottom7	bottom7	90	0.0416514	0.0154052	0.0068780	0.0867740

Reviewer 2(RH) measurements:The MEANS Procedure

Table 2

Variable	Label	N	Mean	Std Dev	Minimum	Maximum
top1	top1	90	0.0242106	0.0102804	0.0068990	0.0550290
top2	top2	90	0.0594703	0.0231563	0.0217510	0.1417450
top3	top3	90	0.0661035	0.0225132	0.0325990	0.1388390
top4	top4	90	0.0523121	0.0198276	0.0201130	0.1488440
top5	top5	90	0.0399806	0.0136377	0.0087260	0.0694410
top6	top6	90	0.0502020	0.0137921	0.0109080	0.0767190
top7	top7	90	0.0732602	0.0123315	0.0490890	0.1048100
bottom1	bottom1	90	0.0594737	0.0184502	0.0101770	0.1169320
bottom2	bottom2	90	0.0326812	0.0140961	0.0063710	0.0685810
bottom3	bottom3	90	0.0260678	0.0117284	0.0075200	0.0559170
bottom4	bottom4	90	0.0552773	0.0242026	0.0158730	0.1144630
bottom5	bottom5	90	0.0796659	0.0358396	0.0288830	0.1798130
bottom6	bottom6	90	0.0683356	0.0277364	0.0238150	0.1534760
bottom7	bottom7	90	0.0416514	0.0154052	0.0068780	0.0867740

Average of Reviewer 1(JB) and Reviewer 2(RH) measurements: The MEANS Procedure

Table 3

Variable	N	Mean	Std Dev	Minimum	Maximum
atop1	90	0.0231911	0.0103755	0.0067015	0.0560860
atop2	90	0.0582850	0.0231521	0.0214080	0.1404405
atop3	90	0.0651931	0.0227452	0.0304300	0.1372995
atop4	90	0.0500862	0.0157916	0.0187225	0.1001735
atop5	90	0.0386566	0.0138782	0.0080480	0.0679410
atop6	90	0.0488460	0.0125053	0.0118030	0.0753975
atop7	90	0.0717831	0.0121340	0.0497400	0.1018760
abottom1	90	0.0587603	0.0187666	0.0090920	0.1203705
abottom2	90	0.0322457	0.0146329	0.0066350	0.0710960
abottom3	90	0.0253499	0.0119799	0.0078925	0.0559170
abottom4	90	0.0541433	0.0237839	0.0156495	0.1134340
abottom5	90	0.0796277	0.0358575	0.0316095	0.1792070
abottom6	90	0.0673275	0.0281630	0.0235695	0.1568970
abottom7	90	0.0401578	0.0150882	0.0063610	0.0841285

Average of Reviewer 1(JB) and Reviewer 2(RH) measurements:
The MEANS Procedure (by Group)

Table 4

Group	N Obs	Variable	N	Mean	Std Dev	Minimum	Maximum
EM	10	atop1	10	0.0174703	0.0086384	0.0069450	0.0341975
		atop2	10	0.0564530	0.0207069	0.0280680	0.0921490
		atop3	10	0.0693279	0.0185718	0.0373760	0.0956525
		atop4	10	0.0513233	0.0116351	0.0364325	0.0701460
		atop5	10	0.0397423	0.0058458	0.0267255	0.0461100
		atop6	10	0.0410929	0.0094025	0.0321200	0.0576915
		atop7	10	0.0617621	0.0030185	0.0568795	0.0672005
		abottom1	10	0.0718705	0.0139381	0.0472825	0.0967115
		abottom2	10	0.0372982	0.0172960	0.0143865	0.0643565
		abottom3	10	0.0153501	0.0064168	0.0084365	0.0294450
		abottom4	10	0.0343563	0.0094619	0.0221475	0.0539900
		abottom5	10	0.0601620	0.0170224	0.0391230	0.0873950
		abottom6	10	0.0614587	0.0213880	0.0265045	0.0942615
		abottom7	10	0.0381680	0.0107408	0.0227775	0.0500030
HF	10	atop1	10	0.0287380	0.0132329	0.0081045	0.0477245
		atop2	10	0.0961797	0.0243475	0.0745905	0.1404405
		atop3	10	0.0955986	0.0184499	0.0743410	0.1372995
		atop4	10	0.0536314	0.0199559	0.0330715	0.1001735
		atop5	10	0.0286398	0.0097825	0.0183740	0.0506565
		atop6	10	0.0431621	0.0146538	0.0118030	0.0655825
		atop7	10	0.0756147	0.0104068	0.0563505	0.0931290
		abottom1	10	0.0827458	0.0172108	0.0613860	0.1203705
		abottom2	10	0.0387665	0.0209237	0.0084140	0.0710960
		abottom3	10	0.0299474	0.0136197	0.0156175	0.0556200
		abottom4	10	0.0875277	0.0244809	0.0316470	0.1134340
		abottom5	10	0.1435174	0.0189232	0.1162985	0.1792070
		abottom6	10	0.1055796	0.0277709	0.0702485	0.1568970
		abottom7	10	0.0448278	0.0162239	0.0296410	0.0817500
K3	10	atop1	10	0.0195490	0.0086201	0.0071995	0.0343960
		atop2	10	0.0344030	0.0079812	0.0214080	0.0460485
		atop3	10	0.0456031	0.0063624	0.0351560	0.0529645
		atop4	10	0.0560155	0.0159665	0.0413900	0.0953050
		atop5	10	0.0537980	0.0085225	0.0416660	0.0658435
		atop6	10	0.0577916	0.0067503	0.0437275	0.0666720
		atop7	10	0.0670712	0.0075216	0.0524000	0.0753965
		abottom1	10	0.0524861	0.0111117	0.0377700	0.0693715
		abottom2	10	0.0338436	0.0111306	0.0187410	0.0539925
		abottom3	10	0.0299268	0.0078463	0.0202080	0.0408030
		abottom4	10	0.0372803	0.0106514	0.0224870	0.0573265
		abottom5	10	0.0443322	0.0088054	0.0345955	0.0591165
		abottom6	10	0.0441545	0.0075208	0.0326085	0.0585385
		abottom7	10	0.0401409	0.0053712	0.0333515	0.0481510

Group	N Obs	Variable	N	Mean	Std Dev	Minimum	Maximum
M4	10	atop1	10	0.0250876	0.0125328	0.0097195	0.0428600
		atop2	10	0.0825536	0.0221021	0.0481920	0.1107235
		atop3	10	0.0818800	0.0251827	0.0507780	0.1135675
		atop4	10	0.0528463	0.0240244	0.0275690	0.0982875
		atop5	10	0.0222753	0.0135049	0.0080480	0.0475865
		atop6	10	0.0430715	0.0127023	0.0259985	0.0608885
		atop7	10	0.0796902	0.0122936	0.0608475	0.1000005
		abottom1	10	0.0647066	0.0103696	0.0494280	0.0820145
		abottom2	10	0.0304096	0.0151700	0.0066350	0.0565995
		abottom3	10	0.0130538	0.0049293	0.0078925	0.0221085
		abottom4	10	0.0728514	0.0189975	0.0277490	0.1008815
		abottom5	10	0.1153147	0.0188428	0.0860975	0.1430055
		abottom6	10	0.0768553	0.0291364	0.0259395	0.1284880
		abottom7	10	0.0328819	0.0150016	0.0063610	0.0584665
PF	10	atop1	10	0.0296436	0.0102408	0.0193105	0.0560860
		atop2	10	0.0568506	0.0083163	0.0427920	0.0678090
		atop3	10	0.0569437	0.0106138	0.0415160	0.0757420
		atop4	10	0.0457078	0.0067565	0.0368125	0.0599125
		atop5	10	0.0432143	0.0074626	0.0318390	0.0541325
		atop6	10	0.0539866	0.0088738	0.0403215	0.0680535
		atop7	10	0.0719380	0.0073901	0.0614220	0.0841275
		abottom1	10	0.0559327	0.0112801	0.0364805	0.0699575
		abottom2	10	0.0239394	0.0108136	0.0085530	0.0410270
		abottom3	10	0.0234775	0.0089208	0.0101640	0.0432425
		abottom4	10	0.0433027	0.0069871	0.0337295	0.0516565
		abottom5	10	0.0605945	0.0093079	0.0476135	0.0776365
		abottom6	10	0.0528132	0.0094635	0.0386495	0.0679355
		abottom7	10	0.0367282	0.0085842	0.0246030	0.0507965
PS	10	atop1	10	0.0221646	0.0078215	0.0109145	0.0338800
		atop2	10	0.0439300	0.0086443	0.0342075	0.0598610
		atop3	10	0.0445878	0.0094205	0.0304300	0.0660680
		atop4	10	0.0427542	0.0095168	0.0288695	0.0569580
		atop5	10	0.0369819	0.0080032	0.0260245	0.0506620
		atop6	10	0.0434696	0.0066588	0.0335185	0.0529170
		atop7	10	0.0647665	0.0064616	0.0497400	0.0701065
		abottom1	10	0.0500028	0.0133162	0.0236150	0.0702990
		abottom2	10	0.0279882	0.0144118	0.0098310	0.0525310
		abottom3	10	0.0165151	0.0073570	0.0091855	0.0338140
		abottom4	10	0.0293922	0.0081526	0.0156495	0.0467225
		abottom5	10	0.0457185	0.0112465	0.0316095	0.0663840
		abottom6	10	0.0411503	0.0135718	0.0235695	0.0642935
		abottom7	10	0.0221561	0.0086928	0.0116525	0.0388905

Group	N Obs	Variable	N	Mean	Std Dev	Minimum	Maximum
SR	10	atop1	10	0.0185918	0.0084724	0.0067015	0.0336960
		atop2	10	0.0456613	0.0067381	0.0371540	0.0577340
		atop3	10	0.0522035	0.0096760	0.0343565	0.0634380
		atop4	10	0.0412793	0.0127717	0.0187225	0.0617980
		atop5	10	0.0374954	0.0142905	0.0153155	0.0592450
		atop6	10	0.0469453	0.0096036	0.0337005	0.0625010
		atop7	10	0.0628236	0.0052008	0.0531760	0.0714645
		abottom1	10	0.0371965	0.0152437	0.0090920	0.0552910
		abottom2	10	0.0296965	0.0123679	0.0085325	0.0483285
		abottom3	10	0.0321897	0.0059938	0.0253440	0.0447720
		abottom4	10	0.0538860	0.0109610	0.0363290	0.0679220
		abottom5	10	0.0667649	0.0143878	0.0416690	0.0873415
		abottom6	10	0.0691195	0.0174981	0.0360490	0.0882510
		abottom7	10	0.0428711	0.0109713	0.0230220	0.0579375
VGP	10	atop1	10	0.0199114	0.0087380	0.0073820	0.0365120
		atop2	10	0.0538652	0.0116884	0.0292350	0.0729775
		atop3	10	0.0868330	0.0153539	0.0587725	0.1072030
		atop4	10	0.0646411	0.0120152	0.0402005	0.0806600
		atop5	10	0.0526798	0.0110734	0.0281355	0.0679410
		atop6	10	0.0622199	0.0109959	0.0466345	0.0753975
		atop7	10	0.0898410	0.0091417	0.0737295	0.1018760
		abottom1	10	0.0441157	0.0088251	0.0342980	0.0661205
		abottom2	10	0.0373932	0.0103439	0.0194060	0.0482565
		abottom3	10	0.0430072	0.0088548	0.0305405	0.0559170
		abottom4	10	0.0805089	0.0102527	0.0570235	0.0931940
		abottom5	10	0.1112284	0.0141616	0.0960435	0.1401640
		abottom6	10	0.0985466	0.0180001	0.0765470	0.1371970
		abottom7	10	0.0644261	0.0120180	0.0507965	0.0841285
X	10	atop1	10	0.0275636	0.0087091	0.0158820	0.0405870
		atop2	10	0.0546689	0.0083058	0.0403525	0.0658655
		atop3	10	0.0537605	0.0065459	0.0394050	0.0605530
		atop4	10	0.0425768	0.0113217	0.0311105	0.0697255
		atop5	10	0.0330832	0.0112588	0.0190880	0.0543000
		atop6	10	0.0478744	0.0143609	0.0290455	0.0647610
		atop7	10	0.0725408	0.0139633	0.0531770	0.0955060
		abottom1	10	0.0697865	0.0157812	0.0471035	0.0910055
		abottom2	10	0.0308765	0.0149704	0.0095490	0.0520325
		abottom3	10	0.0246813	0.0065781	0.0105085	0.0337195
		abottom4	10	0.0481841	0.0094217	0.0336185	0.0657775
		abottom5	10	0.0690165	0.0126213	0.0547035	0.0869690
		abottom6	10	0.0562695	0.0150306	0.0371740	0.0762995
		abottom7	10	0.0392203	0.0089756	0.0283065	0.0539735

Outcomes measure: Deviation for All Samples

Table 5

Variable	N	Mean	Std Dev	Minimum	Maximum
tbdiff1	90	-0.0355693	0.0208799	-0.1113395	0.0108445
tbdiff2	90	0.0260393	0.0289690	-0.0362885	0.1320265
tbdiff3	90	0.0398432	0.0253863	-0.0017265	0.1165980
tbdiff4	90	-0.0040571	0.0284046	-0.0803625	0.0685265
btdiff4	90	0.0040571	0.0284046	-0.0685265	0.0803625
btdiff5	90	0.0409710	0.0426776	-0.0309295	0.1608330
btdiff6	90	0.0184815	0.0344206	-0.0311870	0.1450940
btdiff7	90	-0.0316253	0.0178971	-0.0767085	0.0253995
curve1	90	0.0065640	0.0148749	-0.0341525	0.0510513
curve2	90	0.0079711	0.0236401	-0.0297054	0.0926301

Outcomes measure: Deviation by Group

Table 6

Group	N Obs	Variable	N	Mean	Std Dev	Minimum	Maximum	Lower 95% CL for Mean	Upper 95% CL for Mean
EM	10	tbdiff1	10	-0.0544002	0.0182333	-0.0897665	-0.0343460	-0.0674435	-0.0413568
		tbdiff2	10	0.0191548	0.0351830	-0.0362885	0.0647930	-0.0060136	0.0443233
		tbdiff3	10	0.0539778	0.0231475	0.0161280	0.0856520	0.0374191	0.0705365
		tbdiff4	10	0.0169670	0.0185108	-0.0175575	0.0461230	0.0037252	0.0302088
		btdiff4	10	-0.0169670	0.0185108	-0.0461230	0.0175575	-0.0302088	-0.0037252
		btdiff5	10	0.0204197	0.0193550	-0.0026710	0.0606695	0.0065739	0.0342655
		btdiff6	10	0.0203659	0.0297339	-0.0311870	0.0619090	-0.000904480	0.0416362
		btdiff7	10	-0.0235942	0.0127232	-0.0407455	-0.0092680	-0.0326958	-0.0144925
		curve1	10	0.0089249	0.0175742	-0.0194019	0.0337995	-0.0036469	0.0214967
		curve2	10	0.000056100	0.0144543	-0.0226209	0.0289298	-0.0102839	0.0103961
HF	10	tbdiff1	10	-0.0540078	0.0257739	-0.1113395	-0.0309585	-0.0724454	-0.0355702
		tbdiff2	10	0.0574132	0.0409769	0.0034945	0.1320265	0.0281001	0.0867262
		tbdiff3	10	0.0656512	0.0280883	0.0264555	0.1165980	0.0455581	0.0857443
		tbdiff4	10	-0.0338963	0.0425673	-0.0803625	0.0685265	-0.0643470	-0.0034455
		btdiff4	10	0.0338963	0.0425673	-0.0685265	0.0803625	0.0034455	0.0643470
		btdiff5	10	0.1148777	0.0239694	0.0910855	0.1608330	0.0977310	0.1320243
		btdiff6	10	0.0624175	0.0403187	0.0132725	0.1450940	0.0335753	0.0912597
		btdiff7	10	-0.0307870	0.0240381	-0.0608015	0.0253995	-0.0479828	-0.0135911
		curve1	10	0.0087901	0.0248862	-0.0341525	0.0510513	-0.0090125	0.0265926
		curve2	10	0.0451011	0.0215573	0.0216590	0.0926301	0.0296799	0.0605223
K3	10	tbdiff1	10	-0.0329371	0.0163124	-0.0621720	-0.0037030	-0.0446063	-0.0212679
		tbdiff2	10	0.000559400	0.0173943	-0.0325845	0.0273075	-0.0118837	0.0130025
		tbdiff3	10	0.0156763	0.0095708	0.0028435	0.0327565	0.0088298	0.0225228
		tbdiff4	10	0.0187352	0.0160165	-0.0018460	0.0408305	0.0072777	0.0301927
		btdiff4	10	-0.0187352	0.0160165	-0.0408305	0.0018460	-0.0301927	-0.0072777
		btdiff5	10	-0.0094658	0.0155717	-0.0309295	0.0174505	-0.0206051	0.0016735
		btdiff6	10	-0.0136371	0.0125050	-0.0296375	0.0148110	-0.0225826	-0.0046915
		btdiff7	10	-0.0269303	0.0098627	-0.0417965	-0.0095230	-0.0339857	-0.0198749
		curve1	10	0.000508450	0.0116650	-0.0185374	0.0194061	-0.0078362	0.0088531
		curve2	10	-0.0171921	0.0114755	-0.0297054	0.0026371	-0.0254012	-0.0089830
M4	10	tbdiff1	10	-0.0396191	0.0133937	-0.0532990	-0.0079495	-0.0492003	-0.0300378
		tbdiff2	10	0.0521441	0.0265023	0.0016910	0.0752900	0.0331854	0.0711027
		tbdiff3	10	0.0688262	0.0264044	0.0345795	0.1013120	0.0499376	0.0877148
		tbdiff4	10	-0.0200051	0.0348817	-0.0550630	0.0564380	-0.0449580	0.0049478
		btdiff4	10	0.0200051	0.0348817	-0.0564380	0.0550630	-0.0049478	0.0449580
		btdiff5	10	0.0930395	0.0199991	0.0622940	0.1240710	0.0787329	0.1073460
		btdiff6	10	0.0337838	0.0375829	-0.0293525	0.1024895	0.0068986	0.0606690
		btdiff7	10	-0.0468084	0.0229544	-0.0767085	-0.0023810	-0.0632290	-0.0303877
		curve1	10	0.0153365	0.0162352	-0.0135090	0.0311318	0.0037226	0.0269505
		curve2	10	0.0250050	0.0130206	-0.000158375	0.0397960	0.0156906	0.0343194
PF	10	tbdiff1	10	-0.0262891	0.0189821	-0.0488790	0.0108445	-0.0398681	-0.0127101
		tbdiff2	10	0.0329112	0.0150638	0.0062850	0.0502670	0.0221352	0.0436872
		tbdiff3	10	0.0334662	0.0165301	-0.0017265	0.0561400	0.0216412	0.0452911
		tbdiff4	10	0.0024051	0.0114213	-0.0119810	0.0220230	-0.0057652	0.0105754
		btdiff4	10	-0.0024051	0.0114213	-0.0220230	0.0119810	-0.0105754	0.0057652
		btdiff5	10	0.0173803	0.0135761	-0.0061880	0.0361310	0.0076685	0.0270920
		btdiff6	10	-0.0011734	0.0164359	-0.0226940	0.0258770	-0.0129309	0.0105841
		btdiff7	10	-0.0352099	0.0127020	-0.0547600	-0.0176745	-0.0442963	-0.0261234
		curve1	10	0.0106233	0.0113102	-0.0089998	0.0302369	0.0025325	0.0187142
		curve2	10	-0.0053520	0.0096830	-0.0196021	0.0114073	-0.0122788	0.0015748

Group	N Obs	Variable	N	Mean	Std Dev	Minimum	Maximum	Lower 95% CL for Mean	Upper 95% CL for Mean
PS	10	tbdiff1	10	-0.0278382	0.0141297	-0.0475040	0.0022355	-0.0379460	-0.0177304
		tbdiff2	10	0.0159418	0.0155572	-0.0064810	0.0476510	0.0048128	0.0270707
		tbdiff3	10	0.0280728	0.0116233	0.0061705	0.0499220	0.0197579	0.0363876
		tbdiff4	10	0.0133620	0.0116747	0.0015380	0.0354995	0.0050104	0.0217135
		btdiff4	10	-0.0133620	0.0116747	-0.0354995	-0.0015380	-0.0217135	-0.0050104
		btdiff5	10	0.0087366	0.0145597	-0.0190525	0.0246730	-0.0016789	0.0191520
		btdiff6	10	-0.0023193	0.0177250	-0.0254840	0.0250050	-0.0149989	0.0103604
		btdiff7	10	-0.0426105	0.0105710	-0.0552870	-0.0261885	-0.0501725	-0.0350484
		curve1	10	0.0073846	0.0085358	-0.0085096	0.0229446	0.0012784	0.0134907
		curve2	10	-0.0123888	0.0087020	-0.0267229	0.0027861	-0.0186138	-0.0061638
SR	10	tbdiff1	10	-0.0186048	0.0149237	-0.0391495	0.0045385	-0.0292805	-0.0079290
		tbdiff2	10	0.0159649	0.0148208	-0.0111745	0.0364880	0.0053627	0.0265670
		tbdiff3	10	0.0200139	0.0117269	0.0028790	0.0353380	0.0116250	0.0284027
		tbdiff4	10	-0.0126068	0.0202883	-0.0491995	0.0167350	-0.0271202	0.0019067
		btdiff4	10	0.0126068	0.0202883	-0.0167350	0.0491995	-0.0019067	0.0271202
		btdiff5	10	0.0292696	0.0238905	0.0020150	0.0655680	0.0121793	0.0463598
		btdiff6	10	0.0221742	0.0264168	-0.0245630	0.0545505	0.0032768	0.0410716
		btdiff7	10	-0.0199524	0.0118458	-0.0415335	-0.0052895	-0.0284264	-0.0114784
		curve1	10	0.0011918	0.0118347	-0.0174670	0.0151745	-0.0072742	0.0096578
		curve2	10	0.0110245	0.0169665	-0.0146915	0.0327899	-0.0011126	0.0231617
VGP	10	tbdiff1	10	-0.0242043	0.0087474	-0.0435465	-0.0137540	-0.0304618	-0.0179468
		tbdiff2	10	0.0164720	0.0149254	-0.0022375	0.0444435	0.0057950	0.0271489
		tbdiff3	10	0.0438258	0.0177435	0.0189740	0.0694870	0.0311328	0.0565187
		tbdiff4	10	-0.0158678	0.0189970	-0.0451985	0.0236365	-0.0294574	-0.0022782
		btdiff4	10	0.0158678	0.0189970	-0.0236365	0.0451985	0.0022782	0.0294574
		btdiff5	10	0.0585487	0.0195657	0.0309510	0.0916995	0.0445522	0.0725451
		btdiff6	10	0.0363267	0.0255165	0.0081460	0.0905625	0.0180733	0.0545801
		btdiff7	10	-0.0254150	0.0162314	-0.0410040	0.0029065	-0.0370262	-0.0138037
		curve1	10	0.0050564	0.0112960	-0.0126980	0.0209116	-0.0030243	0.0131371
		curve2	10	0.0213321	0.0149400	0.0011193	0.0486765	0.0106446	0.0320195
X	10	tbdiff1	10	-0.0422230	0.0231859	-0.0743305	-0.0065165	-0.0588091	-0.0256368
		tbdiff2	10	0.0237924	0.0213266	-0.0116800	0.0563165	0.0085363	0.0390485
		tbdiff3	10	0.0290792	0.0084893	0.0186515	0.0487000	0.0230063	0.0351521
		tbdiff4	10	-0.0056073	0.0186760	-0.0346670	0.0340660	-0.0189673	0.0077527
		btdiff4	10	0.0056073	0.0186760	-0.0340660	0.0346670	-0.0077527	0.0189673
		btdiff5	10	0.0359334	0.0199041	0.000963000	0.0614815	0.0216948	0.0501719
		btdiff6	10	0.0083952	0.0275164	-0.0233665	0.0415055	-0.0112889	0.0280792
		btdiff7	10	-0.0333205	0.0206845	-0.0661385	-0.0076665	-0.0481173	-0.0185237
		curve1	10	0.0012603	0.0129962	-0.0213934	0.0178739	-0.0080366	0.0105572
		curve2	10	0.0041538	0.0189991	-0.0284058	0.0295306	-0.0094373	0.0177450

Change in Surface Area

Table 7

Group	N Obs	Variable	N	Mean	Std Dev	Minimum	Maximum
EM	10	PreSA	10	1.73	0.05	1.67	1.82
		PostSA	10	4.19	0.11	4.08	4.40
		chgSA	10	141.86	10.03	125.79	159.33
HF	10	PreSA	10	1.76	0.08	1.67	1.88
		PostSA	10	4.17	0.11	4.04	4.38
		chgSA	10	137.48	12.57	122.33	159.74
K3	10	PreSA	10	1.73	0.05	1.66	1.80
		PostSA	10	4.16	0.16	3.82	4.36
		chgSA	10	140.56	11.08	122.71	155.83
M4	10	PreSA	10	1.75	0.08	1.58	1.85
		PostSA	10	4.14	0.18	3.95	4.55
		chgSA	10	136.38	18.84	119.60	187.96
PF	10	PreSA	10	1.72	0.07	1.60	1.81
		PostSA	10	4.16	0.15	3.96	4.50
		chgSA	10	142.45	13.04	123.83	168.96
PS	10	PreSA	10	1.73	0.07	1.64	1.88
		PostSA	10	4.22	0.11	4.06	4.35
		chgSA	10	143.70	8.78	127.81	155.89
SR	10	PreSA	10	1.72	0.07	1.57	1.81
		PostSA	10	4.17	0.16	3.97	4.46
		chgSA	10	143.24	11.08	127.55	160.24
VGP	10	PreSA	10	1.73	0.06	1.64	1.82
		PostSA	10	4.21	0.16	4.00	4.48
		chgSA	10	143.82	10.23	126.74	159.12
X	10	PreSA	10	1.68	0.06	1.63	1.81
		PostSA	10	4.25	0.18	4.10	4.70
		chgSA	10	153.32	14.72	130.13	185.22
nc	5	PreSA	5	1.76	0.02	1.72	1.79
		PostSA	5	1.76	0.03	1.71	1.78
		chgSA	5	-0.09	0.27	-0.53	0.17
pc	10	PreSA	10	1.75	0.03	1.71	1.79
		PostSA	10	4.10	0.07	4.00	4.23
		chgSA	10	134.60	6.15	127.49	146.45

Appendix II
File System Information

Table 8

File	Manufacturer	Cost/ file	Files/ pack	Cost/ pack	Size/ Taper	Lengths	Cross-section	Rec speed	Rec Torque	Rec glide path
Endomagic	EndoSolutions	$9.70	5	$48.50	.15/02 .20/02	21, 25	Active-circular	350rpm	None	#10
Pathfile	Dentsply	$8.67	6	$52	.13/02 .16/02 .19/02	21,25,31	Square	300rpm	0.6g/Ncm to 5Ncm	#10
PreShaper	Specialized Endo	$6.16	6	$36.95	.14/02 .18/02	21, 25, 31	Square	500rpm	200g-cm	#10
ScoutRace	Brasseler	$9.73	6	$58.40	.10/02 .10/04 .15/02 .10/06 .20/02	21,25	02/square 04&06 triangular	600rpm-900rpm	1N-cm	#10
V-Glide	SSWhite Burs	$9.03	6	$54.15	.13/02 .17/02	21, 25	Parabolic	200-400rpm	Low torque	#10
X-Plorer	Clinician's Choice	$5.99	6	$35.95	.15/01 .20/01 .20/02 .25/02	21, 25	Triangular Square Square Square	400rpm	200-275g-cm	#08-10
K3	Sybron Endo	$10.49	6	$62.95	.15/02 .20/02	21,25,30	Modified S-type	350	None recom	#10-15
Quantec	Sybron Endo	$12.59	5	$62.95	.15/02 .2/02	21,25	S-type	350	None recom	#10-15

Appendix III
File System Characteristics

Cross Sections

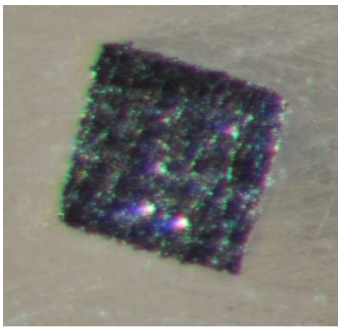

PathFile 16/02

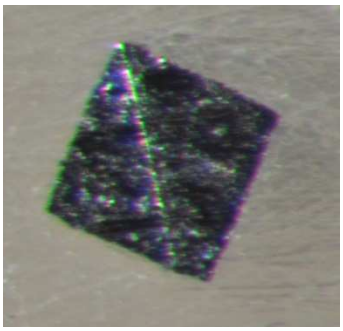

Pre Shaper 14/02

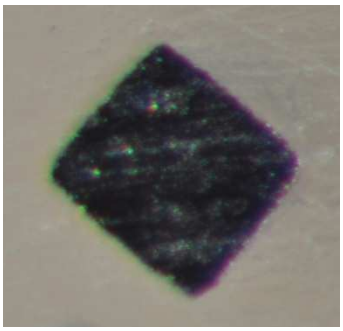

Scout RaCe 15/02

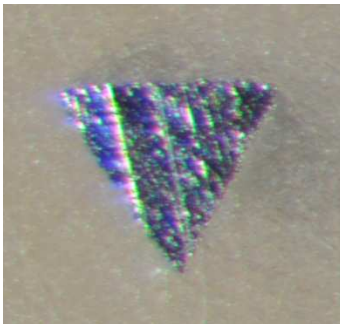

FlexoFile 15/02

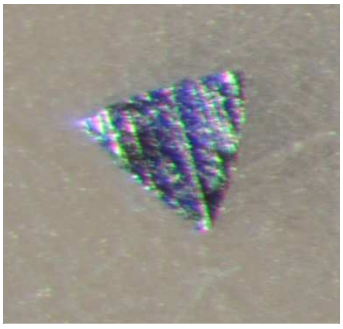

X-Plorer 15/01

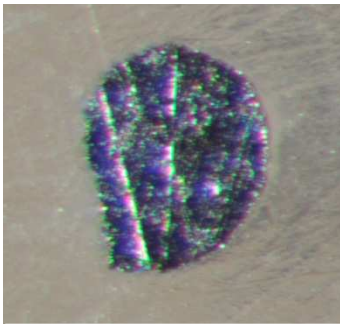

EndoMagic 15/02

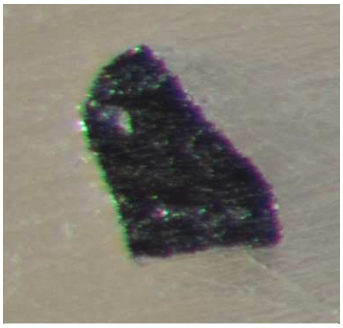

V-Glide 13/02

V-Glide17/02

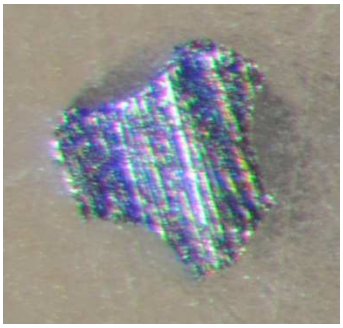

K3 15/02

SEM Images:
EndoMagic (Endo Solutions York, PA)

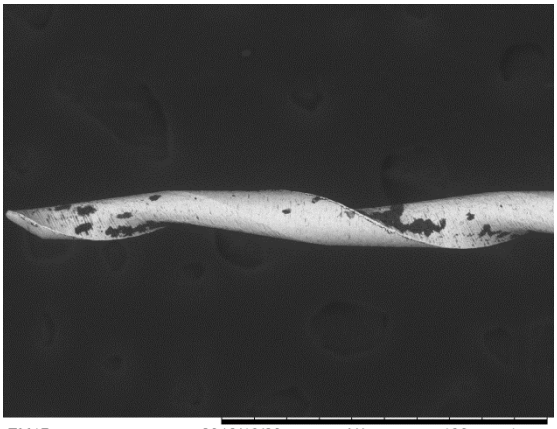

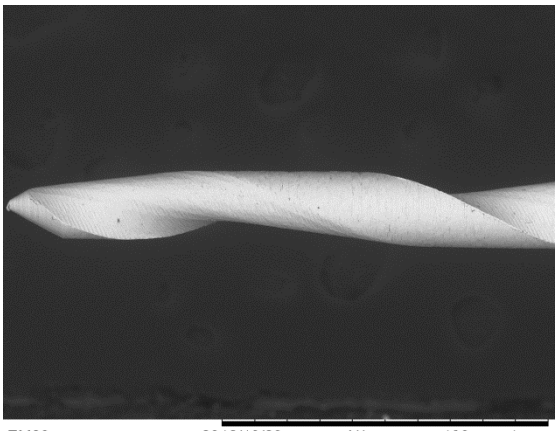

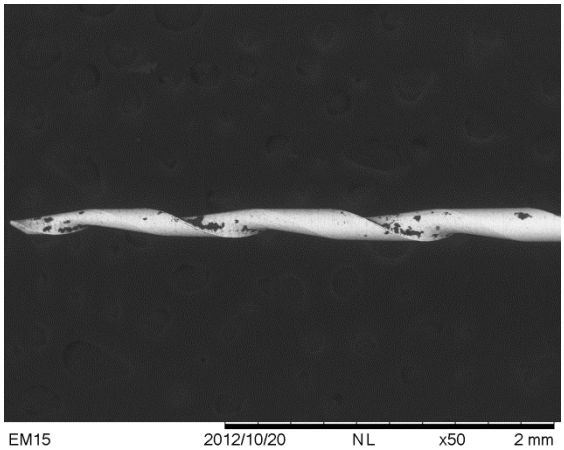

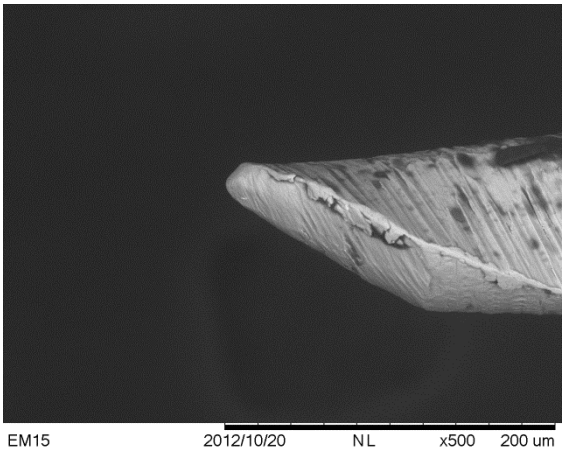

PathFile (Dentsply Maillefer, Tulsa, OK)

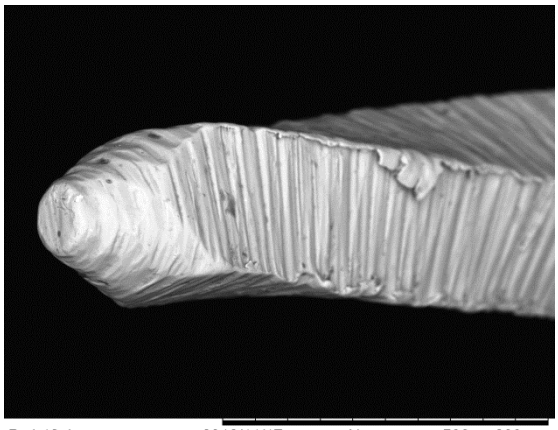

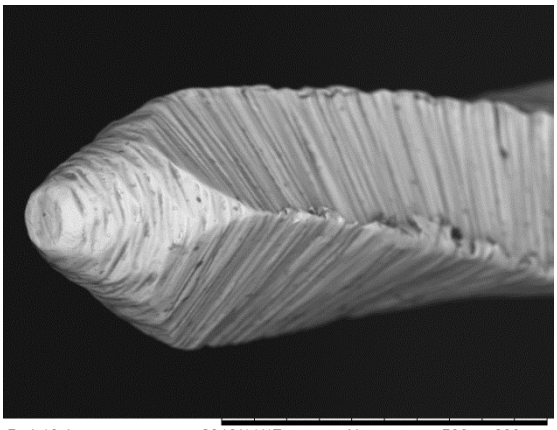

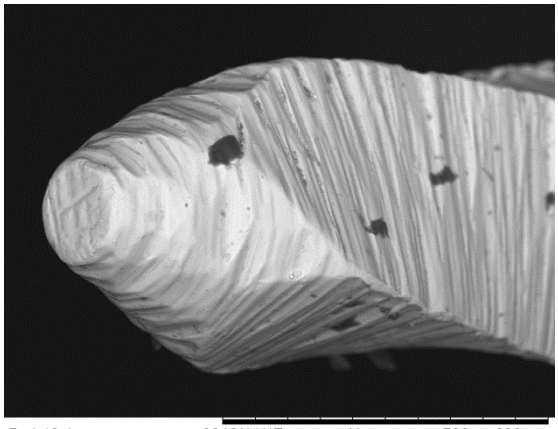

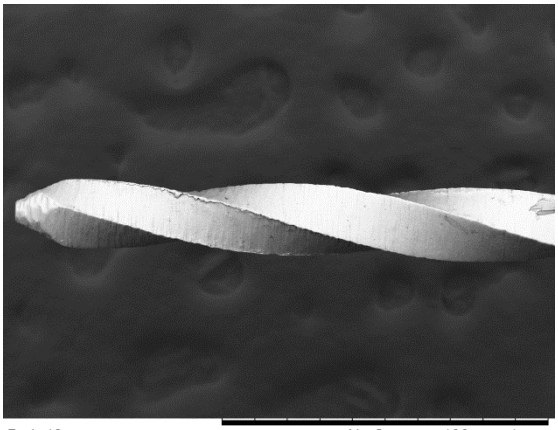

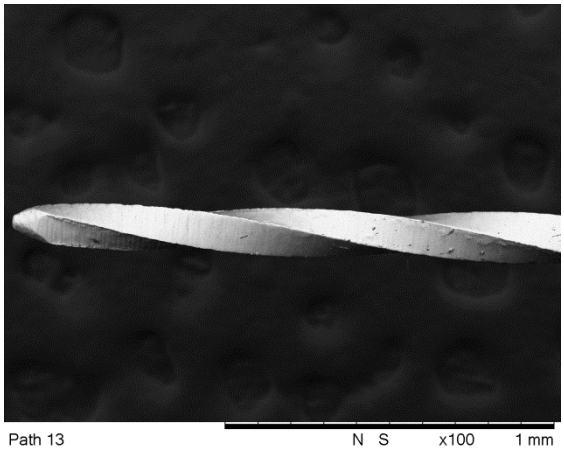

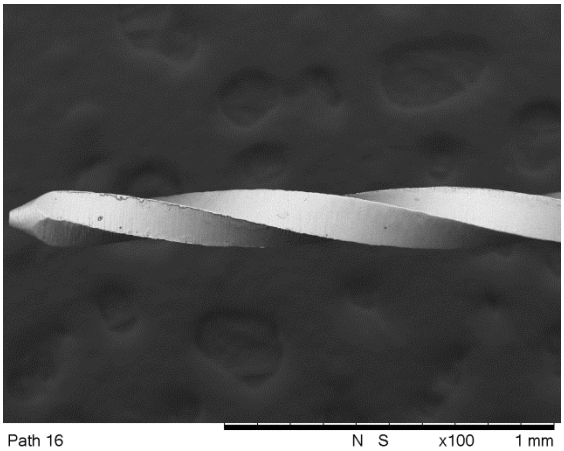

Pre Shaper (Specialized Endo, Portland, OR)

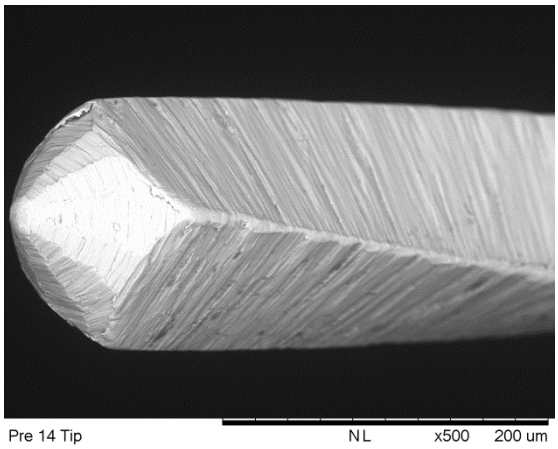

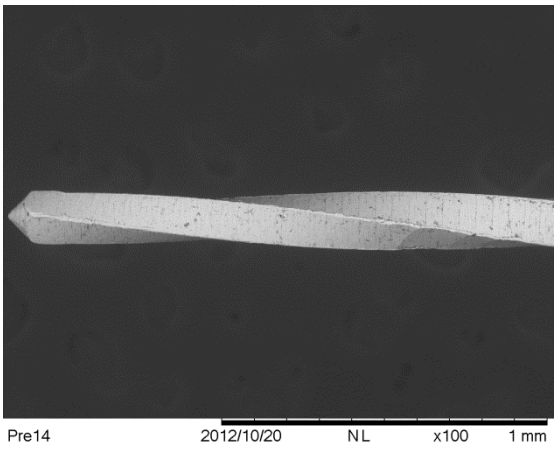

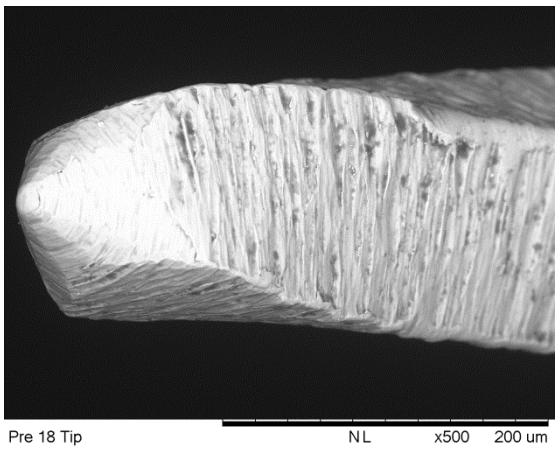

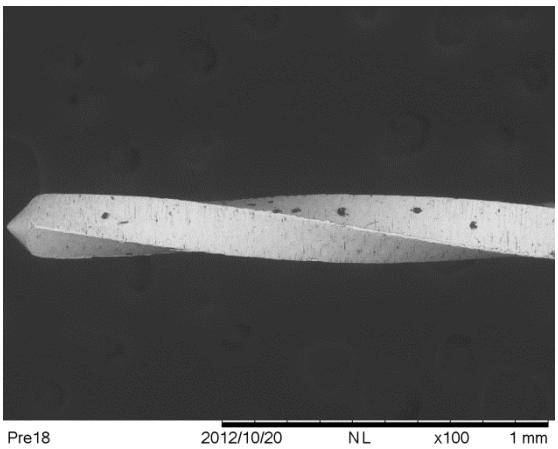

Scout RaCe (Brasseler, Savannah, GA)

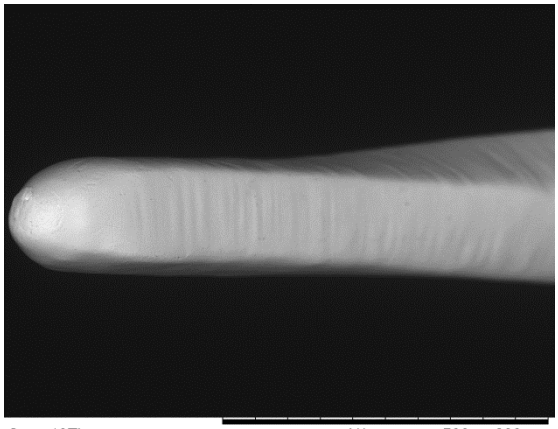

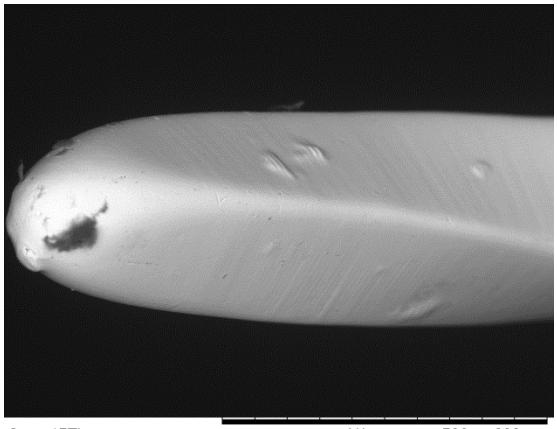

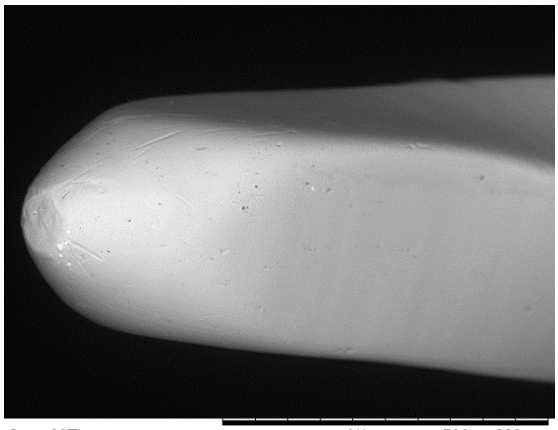

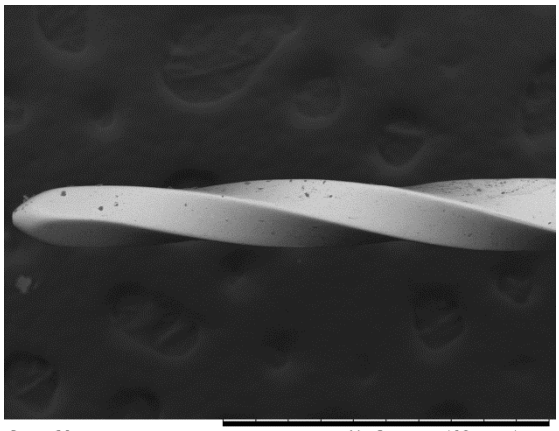

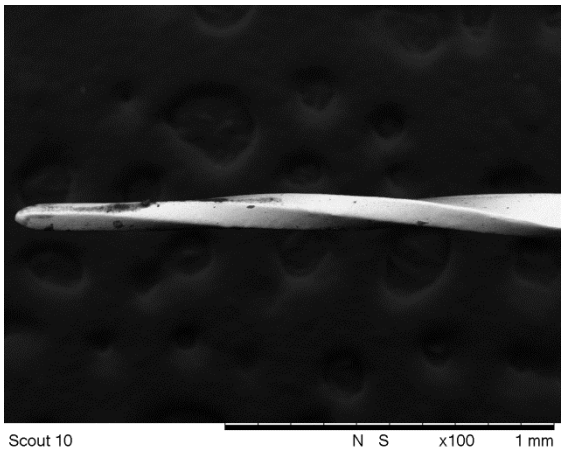

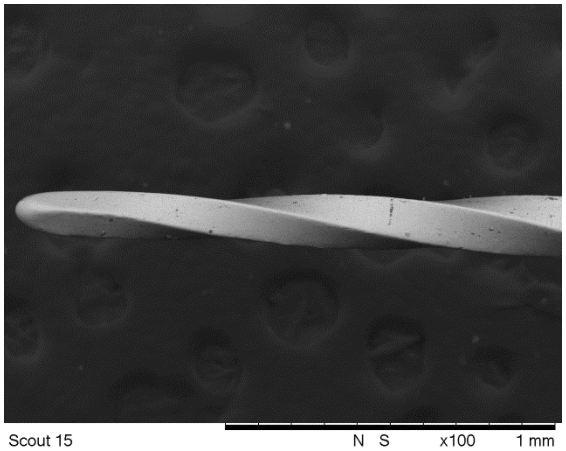

V-Glide (SSWhite, Lakewood, NJ)

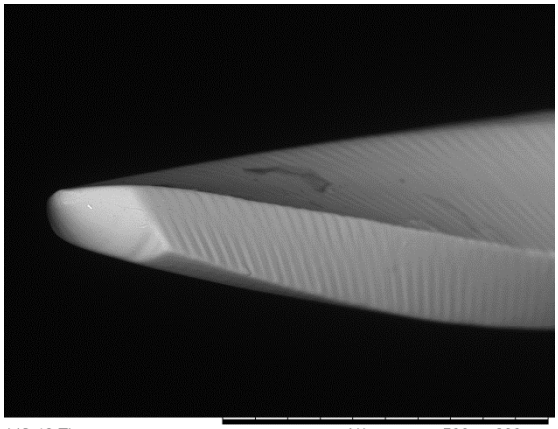

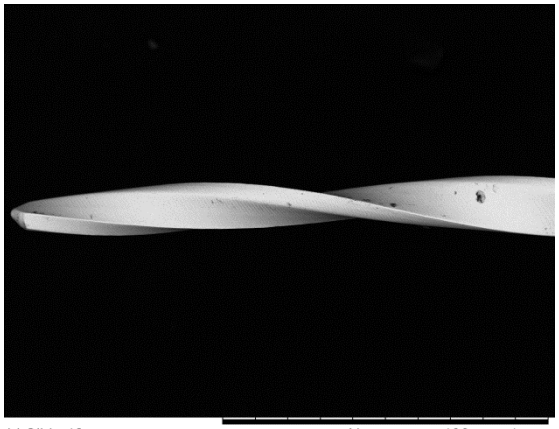

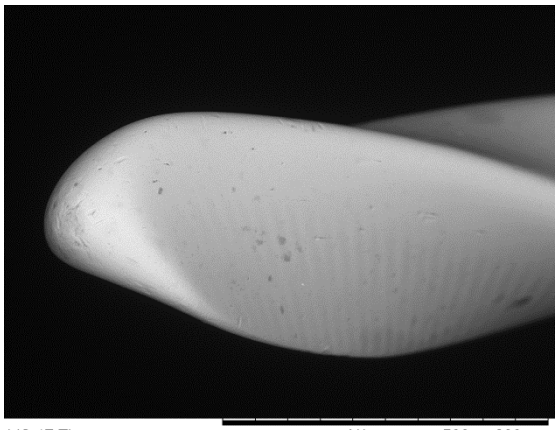

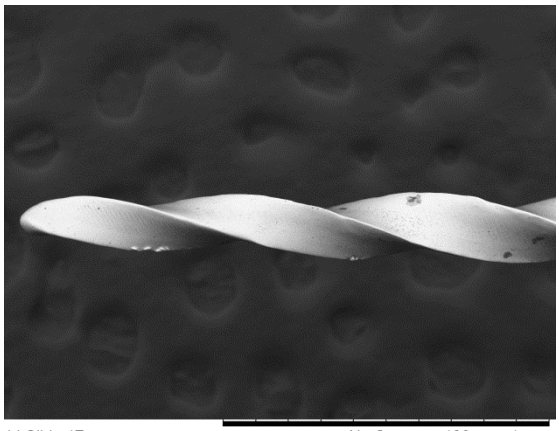

X-plorer (Clinicians Choice, New Milford, CT)

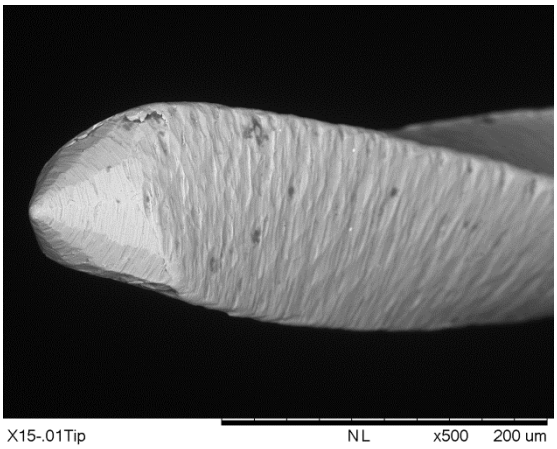

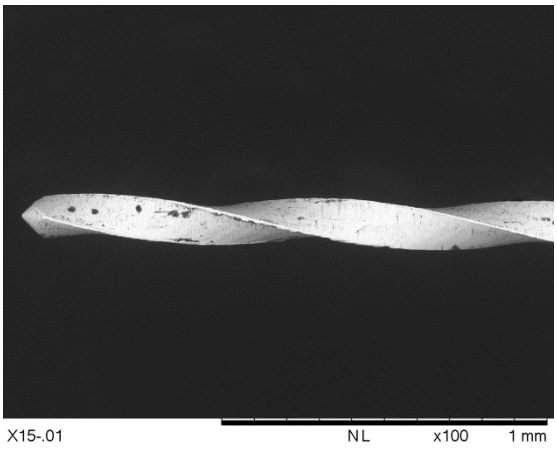

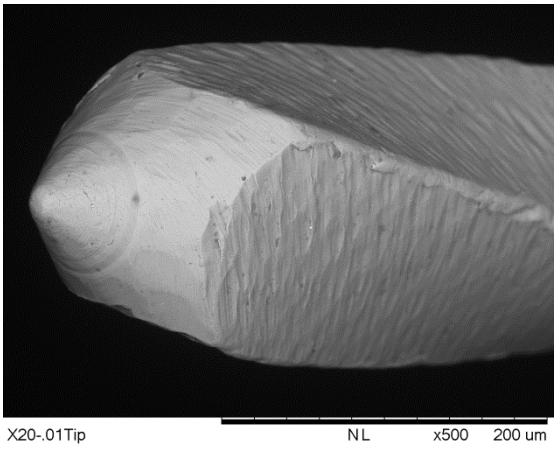

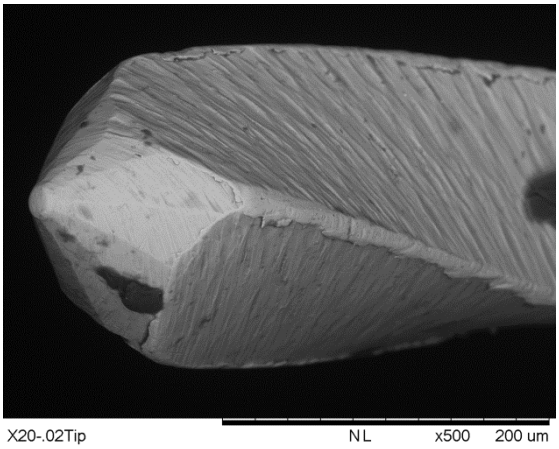

K3 (Sybron, Orange, CA)

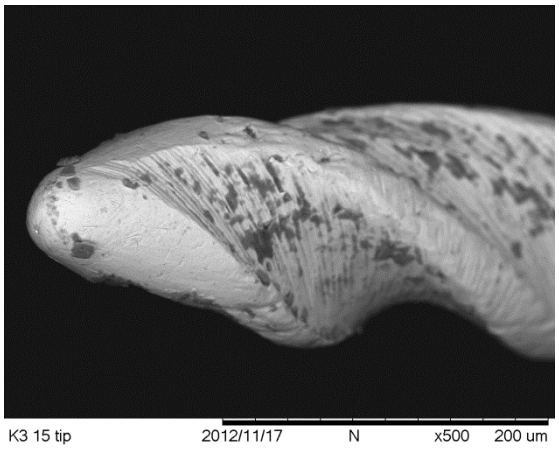

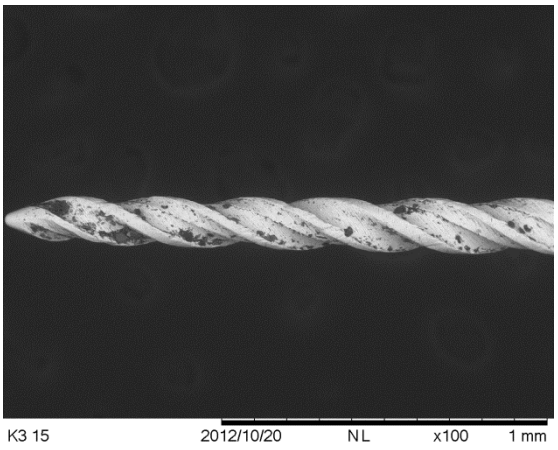

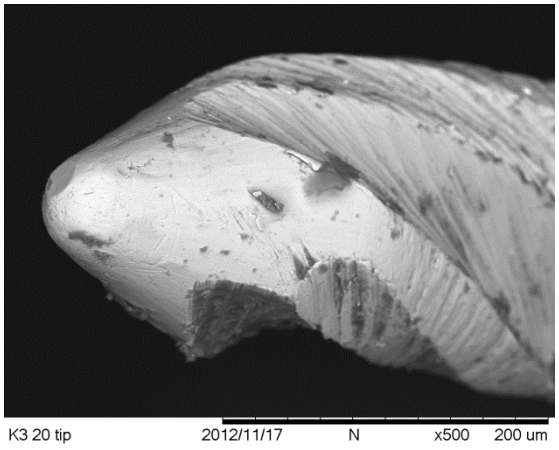

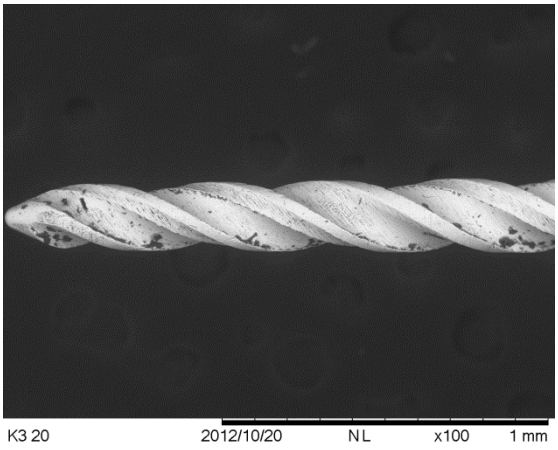

FlexoFile (Hand File) (Dentsply Maillefer, Tulsa, OK)